Bursting oscillations induced by small noise

Pawel Hitczenko and Georgi S. Medvedev [*][†]

September 12, 2021

Abstract

We consider a model of a square-wave bursting neuron residing in the regime of tonic spiking. Upon introduction of small stochastic forcing, the model generates irregular bursting. The statistical properties of the emergent bursting patterns are studied in the present work. In particular, we identify two principal statistical regimes associated with the noise-induced bursting. In the first case, (type I) bursting oscillations are created mainly due to the fluctuations in the fast subsystem. In the alternative scenario, type II bursting, the random perturbations in the slow dynamics play a dominant role. We propose two classes of randomly perturbed slow-fast systems that realize type I and type II scenarios. For these models, we derive the Poincare maps. The analysis of the linearized Poincare maps of the randomly perturbed systems explains the distributions of the number of spikes within one burst and reveals their dependence on the small and control parameters present in the models. The mathematical analysis of the model problems is complemented by the numerical experiments with a generic Hodgkin-Huxley type model of a bursting neuron.

1 Introduction

Differential equation models of excitable cells often include small random terms to reflect the unresolved or poorly understood aspects of the problem or to account for intrinsically stochastic factors [1, 8, 9, 10, 15, 16, 32, 41, 39, 43, 46]. In addition, many neuronal models also exhibit multistability [38, 26]. In systems with multiple stable states, noise may induce transitions between different attractors in the system dynamics, thus, creating qualitatively new dynamical regimes, that are not present in the deterministic system. In the present paper, we study this situation for a class of square-wave bursting models of excitable cell membranes. This class includes many conductance-based models of excitable cell membranes. Here we just mention the model of a pancreatic $\beta-$cell [6, 7], models of neurons in various central pattern generators such as those involved in insect locomotion [20], control of the heartbeat in a leech [25], and respiration in mammals [4, 5], to name a few. These models, as well as the underlying biological systems, exhibit characteristic bursting patterns of the voltage time series: clusters of fast spikes alternating with pronounced periods

---

[*]Department of Mathematics, Drexel University, 3141 Chestnut Street, Philadelphia, PA 19104, phitczen@math.drexel.edu, medvedev@drexel.edu
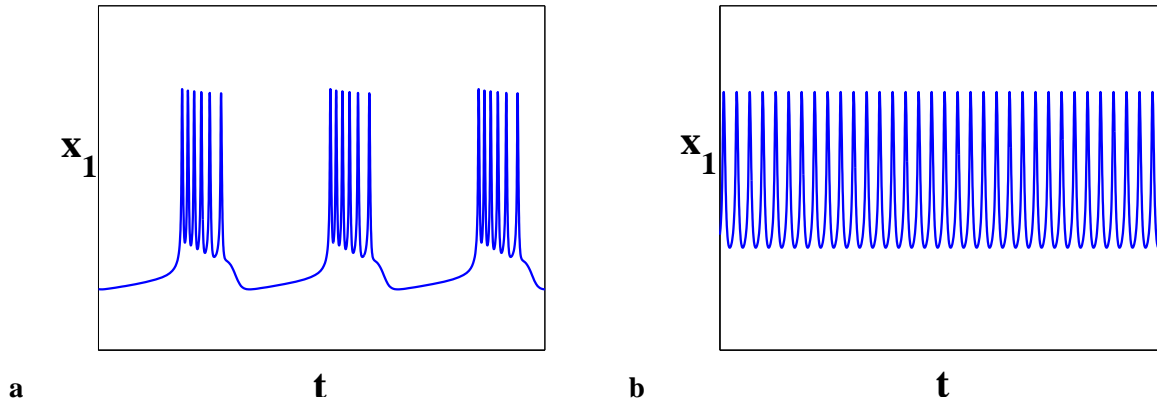
Figure 1: The dynamical patterns generated by a model of of a square-wave bursting neuron (1.1) and (1.2): (a) periodic bursting and (b) tonic spiking.

of quiescence (Fig. 1a). For introduction to bursting, examples and bibliography, we refer the reader to [26, 31, 37, 38]. The dynamical patterns generated by the conductance-based models typically depend sensitively on parameters. For example, models of square-wave bursting neurons often exhibit both bursting and spiking behaviors for different values of parameters (see Fig. 1a,b). In many relevant experiments, the transition from spiking to bursting is achieved by changing the injected current. In the present paper, we consider a model of a square-wave bursting neuron in the regime of tonic spiking (Fig. 1b). We show that a small noise can transform spiking patterns into irregular (noise-induced) bursting patterns and describe two distinct mechanisms for generating noise-induced bursting. In the first scenario, bursting oscillations are triggered by the fluctuations in the fast subsystem. We refer to this mechanism as type I bursting. In contrast, the bursting dynamics in type II scenario are driven by the random motion along the slow manifold. For each of these cases, we describe the statistical properties of the emergent bursting patterns and characterize them in terms of the small and control parameters present in the model.

Noise-induced phenomena have received considerable attention in the context of neuronal modeling (see, e.g., [1, 8, 9, 32, 39, 41, 43, 46]). A representative example is given by a $2D$ excitable system perturbed by the white noise of small intensity [1]. In the presence of noise and under certain general conditions, a typical trajectory occasionally leaves the basin of attraction (BA) of the stable equilibrium and makes a large excursion in the phase plane of the deterministic system before returning to a small neighborhood of the stable fixed point (Fig. 2a). This gives rise to irregular spiking (Fig. 2b). The properties of the noise-induced spiking and stochastic resonance type effects arising in the context of the perturbed FitzHugh-Nagumo model have been considered in [1, 8, 9, 10] (see also [3, 17, 18, 19] for the mathematical analysis of more general classes of related phenomena in randomly perturbed slow-fast systems). In the present paper, we study a related mechanism for irregular bursting. Specifically, we consider a class of models of square-wave bursting neurons:

$$\dot{x} = f(x, y), \tag{1.1}$$
$$\dot{y} = \epsilon g(x, y), \quad x = (x^1, x^2)^T \in \mathbb{R}^2, \ y \in \mathbb{R}^1, \tag{1.2}$$

where f and g are smooth functions and $0 < \epsilon \ll 1$ is a small parameter. We refer to (1.1), where y is
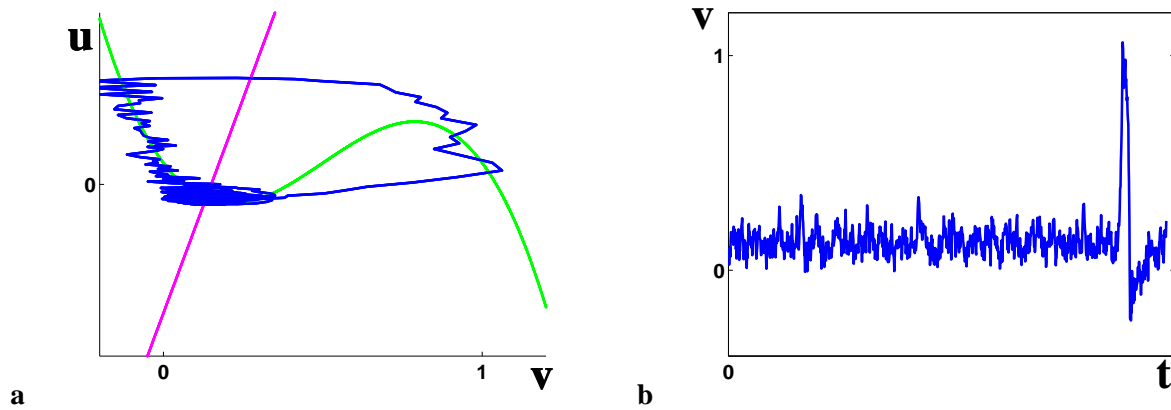
Figure 2: (a) A phase-plane trajectory of the randomly perturbed FitzHugh-Nagumo model in excitable regime (see [1] for the model description and the parameter values). (b) The time series corresponding to the phase plot in (a).

treated as a parameter, as a fast subsystem. It is formally obtained from (1.1) and (1.2) by setting $\epsilon = 0$. We assume that the fast subsystem has a family of stable limit cycles and that of stable equilibria for y in a certain interval $y \in (y_{sn}, y_{bp})$ (see Fig. 3a). The additional assumptions on (1.1) and (1.2), which are explained in Section 2, imply that for small $\epsilon > 0$, (1.1) and (1.2) has a stable limit cycle as shown in Fig. 3c. In the presence of noise, a typical trajectory of the randomly perturbed system will occasionally leave the BA of the limit cycle of the deterministic system to make an excursion along the curve of equilibria of the degenerate system, E (see Fig. 4a). Thus, in analogy to the $2D$ FitzHugh-Nagumo model (Fig. 2a), noise transforms spiking dynamics into irregular bursting. We refer to the latter as noise-induced bursting. In both examples above, irregular spiking (Fig. 2a) or bursting patterns (Fig. 4a,b) are created due to the escape of a trajectory of the randomly perturbed system from the BA of a stable fixed point in the case of spiking or of that of the stable limit cycle in the case of bursting. The statistics of the first exit times can then be related to the properties of the emergent firing patterns such as the frequency of spiking or the distribution of the number of spikes within one burst. Compared to the analysis of the irregular spiking in the randomly perturbed FitzHugh-Nagumo model (Fig. 2), the analysis of the noise-induced bursting faces several additional challenges due to the fact that in the latter case one has to consider the exit problem for the trajectories near a stable limit cycle as opposed to those near a stable equilibrium in the former case. The structure of the BA of the limit cycle combined with the slow-fast character of the vector field determines the main features of the resultant bursting patterns. The description of the principal statistical regimes associated with the noise-induced bursting is the focus of the present paper.

There are general mathematical approaches for analyzing exit problems for stochastic processes generated by randomly perturbed differential equations such as (1.1) and (1.2): the Wentzell-Freidlin theory of large deviations [19] and the geometric theory for randomly perturbed slow-fast systems due to Berglund and Gentz [3]. In this paper we study the vector fields arising in the context of bursting. The specialized structure of this class of problems allows us to keep the analysis of the present paper self-contained and avoid using more technical methods, which are necessary for analyzing more general situations. Our analytical approach is based on the reduction of a randomly perturbed differential equation model to the Poincare

3

map and studying the exit problems for the trajectories of the discrete system. Using maps is quite natural in the context of bursting due to the intrinsic discreteness of bursting patterns imposed by the presence of spikes. Reductions to maps have been very useful for analyzing bursting dynamics in a variety of deterministic models [6, 33, 34, 35, 40]. As follows from the results of the present paper, the first return maps also provide a very convenient and visual representation for the mechanism underlying noise-induced bursting. In particular, we show that the distributions of spikes in one burst in many cases are effectively determined by $1D$ linear randomly perturbed maps. We develop a set of probabilistic techniques for analyzing the dynamics of randomly perturbed $1D$ and $2D$ linear maps such as those arising in the analysis of bursting. The special structure of this class of problems, which is motivated by the applications to bursting affords a more direct and simpler analysis than the treatment of more general classes of random linear maps found in the literature [29, 21, 28, 45].

The outline of the paper is as follows. In section 2, we formulate our assumptions on the deterministic system. We then present the preliminary numerical results, motivating our formulation of the randomly perturbed models at the end of this section. Specifically, we distinguish two types of the noise-induced bursting. *Type I* bursting is generated due to the fluctuations predominantly in the fast subsystem, while *type II* bursting is induced by variability mainly in the slow variable. Accordingly, we introduce two types of models that generate type I and type II bursting patterns. Section 3 develops a set of probabilistic techniques, which will be needed for the analysis of the first return maps for the randomly perturbed differential equation models. We first analyze a simple linear map with an attracting slope and small additive Gaussian perturbations in Section 3.2. Due to the simple structure of the map, we obtain very explicit characterization of the first exit times for this problem. The analysis of this first relatively simple example provides the guidelines for the more complex cases dealt in Sections 3.3-3.5. Section 4 contains the definition and the construction of the Poincare map for the type I randomly perturbed model introduced in Section 2. The $2D$ Poincare map is decomposed into two $1D$ maps for the fast and slow subsystems, which are constructed in Sections 4.2 and 4.3 respectively. In Section 4.4, we apply the results of Section 3 to the linearization of the Poincare map to derive the distributions of the first exit times. The latter are interpreted as the distributions of the number of spikes in one burst. In Sections 4.5, we outline the modifications necessary to cover type II models. Since the analysis for type II models closely follows the lines of that for type I models, we omit most of the details. Finally, the numerical experiments in Section 5 are designed to illustrate our theory.

2 The model

In the present section, we introduce the model to be studied in the remainder of this paper. We start by formulating our assumptions on the deterministic model and then describe the random perturbation.

2.1 The deterministic model

We consider slow-fast system (1.1) and (1.2) in $\mathbb{R}^3$ with one *slow* variable. The *fast* subsystem associated with (1.1) and (1.2) is obtained by sending $\epsilon \to 0$ in (1.2) and treating y as a parameter:
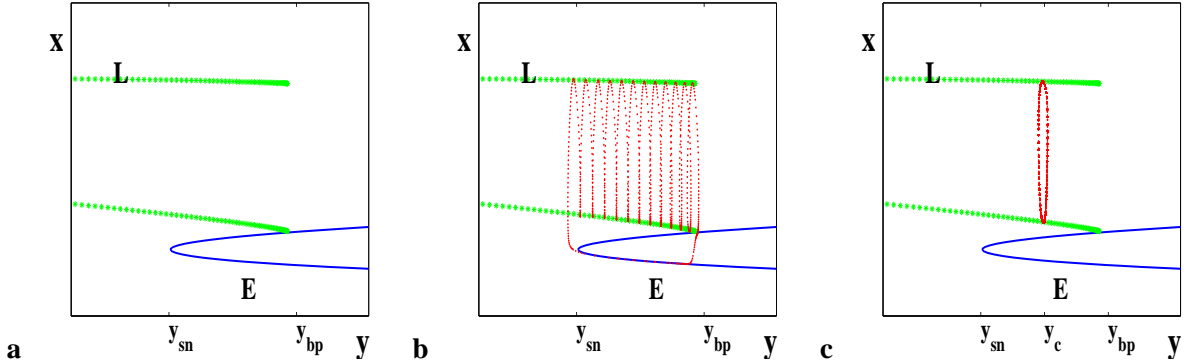
$$\dot{x} = f(x, y). \tag{2.1}$$

Figure 3: (a) The bifurcation diagram of the fast subsystem (2.1). L denotes a cylinder foliated by the stable periodic orbits. The lower branch of the parabolic curve E is composed of stable equilibria of the fast subsystem (see Fig. 6b for the plot of a representative phase plane of the fast subsystem for $y \in (y_{sn}, y_{bp})$). (b,c) Periodic trajectories of the full system (1.1) and (1.2) are superimposed on the bifurcation diagram of the fast subsystem. Assumptions (SE) and (SB) (see the text) result in a bursting limit cycle plotted in red in (b), while (SS) yields spiking (c).

Under the variation of y, the fast subsystem has the bifurcation structure as shown schematically in Fig. 3a. Specifically, we rely on the following assumptions:

(PO) There exists $y_{bp} \in \mathbb{R}$ such that for each $y < y_{bp}$, Equation (2.1) has an exponentially stable limit cycle of period $\mathcal{T}(y)$:

$$L(y) = \{x = \phi(s, y): \ 0 \le s < \mathcal{T}(y)\}. \tag{2.2}$$

The family of the limit cycles, $L = \bigcup_{y < y_{bp}} L(y)$, forms a cylinder in $\mathbb{R}^3$ (Fig. 3a).

(EQ) There is a branch of asymptotically stable equilibria of (2.1), $E = \{x = \psi(y): \ y > y_{sn}\}$, which terminates at a saddle-node bifurcation at $y = y_{sn} < y_{bp}$ (Figure 3a).

(LS) For each $y \in \mathbb{R}$, the $\omega-$limit set of almost all trajectories of (2.1) belongs to $L(y) \bigcup \{\psi(y)\}$.

Remark 2.1. At $y = y_{bp}$, L, either terminates or $L(y_{bp} + 0)$ looses stability. We do not specify the type of the bifurcation at $y = y_{bp}$. It may be, for instance, a homoclinic bifurcation as shown in Fig. 3a, or a saddle-node bifurcation of limit cycles [22].

Having specified the assumptions on the bifurcation structure of the fast subsystem, we turn to the slow dynamics. The geometric theory for singularly perturbed systems implies the existence of the exponentially stable locally invariant manifolds E_ϵ and L_ϵ, which are $O(\epsilon)$ close to $E \bigcap \{(x, y) : y > y_{sn} + \delta\}$ and $L \bigcap \{(x, y) : y < y_{bp} - \delta\}$, respectively, for arbitrary fixed $\delta > 0$ and sufficiently small $\epsilon > 0$ [14, 27]. Manifolds E_ϵ and L_ϵ are called *slow manifolds*. For small $\epsilon > 0$, the dynamics of (1.1) and (1.2) on the slow manifolds is approximated by

$$L_\epsilon : \qquad \dot{y} = \epsilon G(y), \qquad y < y_{bp} - \delta, \tag{2.3}$$

$$E_\epsilon : \qquad \dot{y} = \epsilon g(\psi(y), y), \quad y > y_{sn} + \delta, \tag{2.4}$$

5

where

$$G(y) = \frac{1}{\mathcal{T}(y)} \int_0^{\mathcal{T}(y)} g\left(\phi(s), y\right) ds. \tag{2.5}$$

We distinguish two types of the asymptotic behavior of solutions of (1.1) and (1.2): *bursting* and *spiking* (see Fig. 1). The following conditions on the slow subsystem yield bursting.

For some $c > 0$ independent of ϵ,

(SE)

$$g(\psi(y), y) < -c \quad \text{for} \quad y > y_{sn}, \tag{2.6}$$

(SB)

$$G(y) > c \quad \text{for} \quad y < y_{bp}. \tag{2.7}$$

Under these assumptions, for sufficiently small $\epsilon > 0$ a typical trajectory of (1.1) and (1.2) consists of the alternating segments closely following L_ϵ and E_ϵ and fast transitions between them (see Fig. 3b). For detailed discussions of the geometric construction of 'bursting' periodic orbits, we refer the reader to [31, 37]. To obtain spiking, we substitute (SB) with

(SS) $G(y)$ has a unique simple zero at $y = y_c \in (y_{sn}, y_{bp})$:

$$G(y_c) = 0 \quad \text{and} \quad G'(y_c) < 0. \tag{2.8}$$

In this case, the asymptotic behavior of solutions follows from the following theorem due to Pontryagin and Rodygin:

Theorem 2.2. *[36] If $\epsilon > 0$ is sufficiently small, (1.1) and (1.2) has a unique exponentially stable limit cycle $L_\epsilon(y_c)$ of period $\mathcal{T}(y_c) + O(\epsilon)$ lying in an $O(\epsilon)$ neighborhood of $L(y_c)$, provided (SS) holds.*

Almost all trajectories of (1.1) and (1.2) are attracted by the limit cycle lying in an $O(\epsilon)$ neighborhood of $L(y_c)$. This mode of behavior is called spiking (see Fig. 3c and Fig. 3b). In the remainder of this paper we assume (SS), in addition, to (PO), (EQ), (LS), and (SE).

2.2   The randomly perturbed models

In this subsection, we provide a heuristic description of the effects of the random perturbations on the dynamics of (1.1) and (1.2). To study these effects quantitatively, at the end of this section, we propose two randomly perturbed models.

Suppose the trajectories of (1.1) and (1.2) experience weak stochastic forcing, such that the perturbed trajectories represent well-defined stochastic processes and are close to the trajectories of (1.1) and (1.2) on finite intervals of time. Since the trajectories of the unperturbed system remain in a small neighborhood
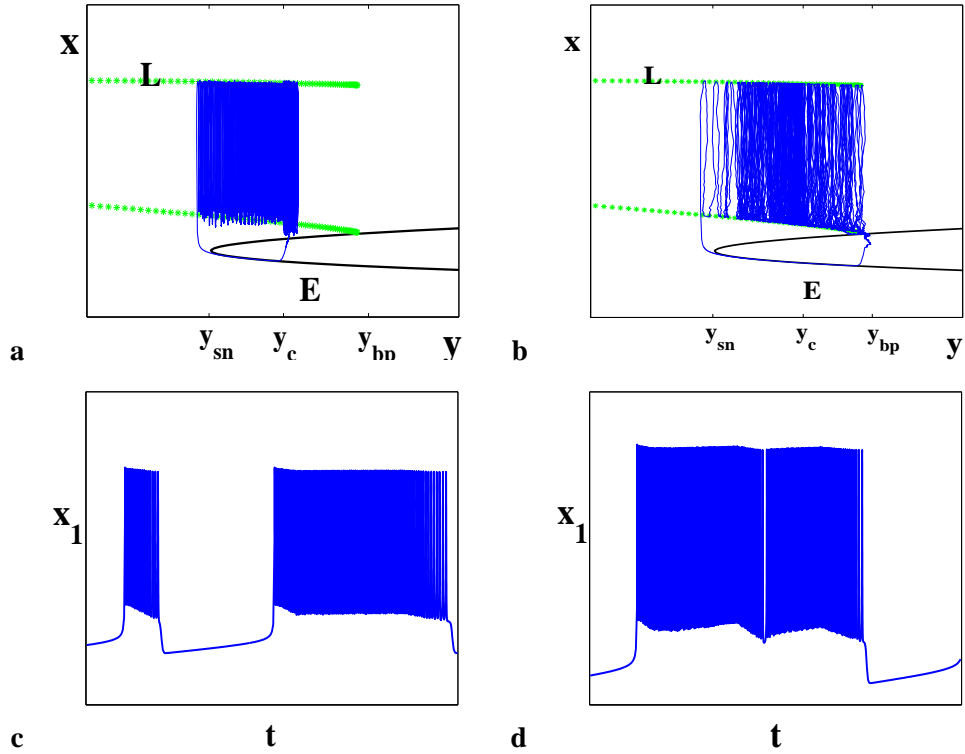
Figure 4: Noise-induced bursting. (a) A trajectory of the randomly perturbed system is shown in the phase space of the frozen system (1.1), (1.2) with $\epsilon = 0$. The trajectory leaves the basin of $L(y_c)$ mainly due to the fluctuations in the fast plane. This is characteristic to *type I* bursting. An alternative *type II* scenario is shown in plot (b), where the fluctuations in the slow direction dominate in the mechanism of escape from the basin of the stable limit cycle. The trajectory in (b) samples a wide region of L and leaves a neighborhood of L near the right boundary, $y \approx y_{bp}$; while that in (a) remains near $L(y_c)$ most of the time and jumps down near $y \approx y_c$. The differences translate into the distinctive features of the generic time series of the bursting patterns generated via type I or type II mechanisms shown in plots (c) and (d) respectively. Note that the longer burst in (c) has a typical square-wave form (roughly, determined by $L(y_c)$), while the burst shown in (d) exhibits more variability due to the drifting of the trajectory along L.

of $L(y_c)$ (possibly after short transients), we expect that in the presence of noise the trajectories will occasionally leave the BA of $L(y_c)$ and after making a brief excursion along E will return back to the vicinity of $L(y_c)$. Therefore, under random perturbation the system can exhibit bursting dynamics, while the underlying deterministic system is in the spiking regime. We refer to this mode of behavior as *noise-induced* bursting. Our goal is to describe typical statistical regimes associated with the noise-induced bursting and to relate them to the structure of (1.1) and (1.2) and to the properties of the stochastic forcing. To illustrate the implications of the structure of the deterministic vector field for the bursting patterns that it produces under random perturbations, we refer to the following numerical examples. Note that the BA of $L(y_c)$ naturally extends along the cylinder of periodic orbits L (Fig. 3c). The escape from the BA of $L(y_c)$ can be dominated by the fluctuations along L or by those in the transverse plane. These two possibilities are shown in Fig. 4. The trajectory shown in Fig. 4a spends most of the time near $L(y_c)$ and leaves its BA due to the fluctuations in the fast subsystem. We refer to this scenario as *type I* escape. Alternatively, the trajectory shown in Fig. 4b travels a good deal along L before the escape and exits from the BA near $y = y_{bp}$. This mechanism is dominated by the slow dynamics. We refer to this scenario as *type II* escape. These mechanisms of escape translate into distinct features of the resultant bursting patterns. First, note that since in type I and type II scenarios, the transition from spiking to quiescence typically takes place at $y \approx y_c$ and $y \approx y_{bp}$ respectively, by (1.2) and (EQ), the corresponding interburst intervals are approximately equal to

$$IBI \approx \epsilon^{-1} \int_{\hat{y}}^{y_{sn}} \frac{dy}{g\left(\psi(y), y\right)}, \quad \text{where} \quad \begin{cases} \hat{y} = y_c, & \text{type I}, \\ \hat{y} = y_{bp}, & \text{type II}. \end{cases}$$

In addition, we expect that the interspike intervals (ISIs) within one burst in type I scenario are localized about $\mathcal{T}(y_c)$, since the trajectory of the randomly perturbed system in the active phase of bursting spends most of the time near $L(y_c)$. In type II bursting patterns, ISIs are expected to have more variability, since the trajectories sample a wider range of ISIs during their excursions along L. Perhaps, a more pronounced distinction between these two types of bursting patterns lies in the degree of the variability of the spikes in one burst. Most of the spikes forming a burst in type I pattern are generated by (2.1) with $y \approx y_c$ and, therefore, are similar in shape (Fig. 4c). In contrast, spikes in type II scenario are subject to more variability and the bursting patterns typically have ragged shape (Fig. 4d).

To study type I and type II noise-induced bursting patterns it is convenient to consider two types of models. *Type I model* incorporates random forcing in the fast subsystem:

$$\dot{x}_t = f\left(x_t, y_t\right) + \sigma p \dot{w}_t, \tag{2.9}$$
$$\dot{y}_t = \epsilon g(x_t, y_t), \tag{2.10}$$

while, in *type II model* the slow subsystem is forced

$$\dot{x}_t = f\left(x_t, y_t\right), \tag{2.11}$$
$$\dot{y}_t = \epsilon\left(g(x_t, y_t) + \sigma q \dot{w}_t\right). \tag{2.12}$$

Here, $0 < \sigma \ll 1$, $p(x, y) = \left(p^1(x, y), p^2(x, y)\right)^T$ and $q(x, y)$ are differentiable functions; $\dot{w}_t$ stands for the white noise, i.e. a generalized derivative of the Wiener process.

8

3 The randomly perturbed maps

In this section, we develop probabilistic tools needed for the analysis of randomly perturbed systems (2.9)-(2.12). The number of spikes in one burst is a natural random variable associated with the noise-induced bursting. It is commonly used in the experimental studies of bursting and we shall adopt it for characterizing irregular bursting patterns in this work. In Section 4, we will show that the number of spikes in one burst is represented by a stopping time (more precisely, the level exceedance time) of a discrete random process, the Poincare map of the randomly perturbed system (2.9)-(2.12). In preparation for the analysis of the linearized Poincare map in Section 4, in the present section we study certain stochastic linear difference equations. The equations of this form equations have been considered in the literature before. The study was initiated by Kesten [29] who considered multidimensional case (in which the coefficients of the stochastic equations are random matrices). Subsequent work focused mostly on the $1D$ case. We refer the reader to the papers [21, 45], which contain representative results, examples of applications, and further references. There is also a review paper [12], unfortunately not easily accessible. The convergence properties of the solutions that we will need could be deduced from a general theory of stochastic difference equations. However, the results in the literature are often stated in the most general form and some of the proofs are rather involved. We will be dealing with special cases that are much easier to justify. For this reason, and also to keep the paper self-contained we will include the proofs of the needed results.

3.1 Geometric random variables

We begin by recalling the necessary properties of geometric random variables (RVs). Recall that Y is a geometric RV with parameter p, $0 < p < 1$ if

$$\mathbb{P}\left(Y = k\right) = p(1-p)^{k-1}, \quad k \geq 1. \tag{3.1}$$

We refer the reader to [28, Chapter 5] for the review of the properties of geometric distributions and their applications. In particular, the following characterization of geometric RVs is classical.

Lemma 3.1. *Let Y be a RV with values in the set of positive integers. Y is a geometric with parameter p, $0 < p < 1$, iff*

$$\mathbb{P}(Y = n) = p\mathbb{P}(Y \geq n), \quad n \geq 1. \tag{3.2}$$

Lemma 3.1 motivates the following definition:

Definition 3.2. *Let Y be a random variable with values in the set of positive integers and let $0 < p < 1$. We say that Y is asymptotically geometric with parameter p if*

$$\lim_{n \to \infty} \frac{\mathbb{P}\left(Y = n\right)}{\mathbb{P}(Y \geq n)} = p. \tag{3.3}$$

3.2 The randomly perturbed map: additive perturbation

Consider

$$Y_n = \lambda Y_{n-1} + \varsigma r_n, \quad n \geq 1, \tag{3.4}$$

where $r_1, r_2, \ldots$ are independent identically distributed (IID) copies of the standard normal RV, and Y_0 is a real number. We will use $N(\mu, \eta^2)$ notation for a normal RV with mean μ, variance η^2, and probability density function given by

$$\frac{1}{\sqrt{2\pi}\eta} \exp\left\{-\frac{(x-\mu)^2}{2\eta^2}\right\}, \quad -\infty < x < \infty.$$

We will also let Z denote a generic $N(0,1)$ RV and we will write

$$\Phi(x) := \frac{1}{\sqrt{2\pi}} \int_{-\infty}^{x} e^{-t^2/2} dt,$$

for its distribution function. For a given $h > 0$, let

$$\tau = \inf\{k \geq 1 : Y_k > h\}.$$

Theorem 3.3. *Let*

$$\varepsilon \in (0,1), \quad \lambda = 1 - \varepsilon, \quad \beta^2 = \frac{\varsigma^2}{\varepsilon(2-\varepsilon)}, \quad \text{and} \quad h - Y_0 > 0. \tag{3.5}$$

Then for sufficiently small $\varsigma > 0$, τ is asymptotically geometric RV with parameter

$$p = \frac{1}{\sqrt{2\pi}} \frac{\beta}{h\Phi(h/\beta)} \exp\left\{-\frac{h^2}{2\beta^2}\right\} \left(1 + O\left(\frac{\varsigma}{\varepsilon}\right)^2\right). \tag{3.6}$$

We precede the proof of the theorem with the auxiliary

Lemma 3.4. *For $n \geq 1$, Y_n is a normal RV with*

$$\mathbb{E}\, Y_n = \lambda^n Y_0 \quad \text{and} \quad \text{var}\, Y_n = \frac{\varsigma^2\left(1 - \lambda^{2n}\right)}{1 - \lambda^2} =: \beta_n^2. \tag{3.7}$$

In particular,

$$Y_n \xrightarrow{d} Y \overset{d}{=} N(0, \beta^2),$$

where $\xrightarrow{d}$ (and $\overset{d}{=}$) denote the convergence (equality) in distribution.

Proof (Lemma 3.4): The statements in (3.7) are verified by a straightforward calculation. The rest follows, because $\mathbb{E}\, Y_n \to 0$ and $\beta_n \to \beta$.

Proof (Theorem 3.3): Let $Y_k^* = \max\{Y_j : 1 \leq j \leq k\}$, $k \geq 1$. Then

$$
\begin{aligned}
\mathbb{P}(\tau = n+1) &= \mathbb{P}(Y_{n+1} > h, Y_n^* \leq h) = \mathbb{P}(Y_{n+1} > h | Y_n^* \leq h)\mathbb{P}(Y_n^* \leq h) \\
&= \mathbb{P}(Y_{n+1} > h | Y_n \leq h, Y_{n-1} \leq h, \ldots, Y_0 \leq h)\mathbb{P}(\tau \geq n+1) \\
&= \mathbb{P}(Y_{n+1} > h | Y_n \leq h)\mathbb{P}(\tau \geq n+1). \tag{3.8}
\end{aligned}
$$

10

In the last equality, we used the fact that $\{Y_n\}$ is a Markov process which is clear from (3.4). By (3.8),

$$p_n := \frac{\mathbb{P}(\tau = n+1)}{\mathbb{P}(\tau \geq n+1)} = \mathbb{P}(Y_{n+1} > h \,|\, Y_n \leq h) = \frac{\mathbb{P}(Y_{n+1} > h, Y_n \leq h)}{\mathbb{P}(Y_n \leq h)}. \tag{3.9}$$

In accordance with Definition 3.2, we need to show that $\{p_n\}$ converges and to estimate the limit. By Lemma 3.4,

$$\mathbb{P}(Y_n \leq h) \longrightarrow \Phi(h/\beta), \quad \text{as } n \to \infty.$$

Next, we turn to estimating the numerator in (3.9). We have

$$\begin{aligned}
Q_n &:= \mathbb{P}(Y_{n+1} > h, Y_n \leq h) = \mathbb{P}(\lambda Y_n + \varsigma r_{n+1} > h, Y_n \leq h) \\
&\to \mathbb{P}(\lambda Y + \varsigma Z > h, Y \leq h) =: Q,
\end{aligned}$$

where Z is standard normal, Y is $N(0, \beta^2)$ and they are independent. This follows from Lemma 3.4 and the fact that r_{n+1} is $N(0,1)$ and is independent of Y_n. Q is the probability that a 2D Gaussian vector is in the region $[h, \infty) \times (-\infty, h]$. There are several ways of estimating this probability. We take the following, elementary approach. Let $X = h - Y$ so that X is $N(h, \beta^2)$ and is independent of Z. Then

$$Q = \mathbb{P}\left(Z > \frac{\varepsilon}{\varsigma}h + \frac{1-\varepsilon}{\varsigma}X, X \geq 0\right) = \frac{1}{\sqrt{2\pi}\beta} \int_0^\infty \mathbb{P}\left(Z > \frac{\varepsilon h + (1-\varepsilon)s}{\varsigma}\right) e^{\frac{-(s-h)^2}{2\beta^2}} ds.$$

By the well–known asymptotics (see [13, Ch. VII, Lemma 2 and Sec. 7, Problem 1])

$$\mathbb{P}(Z > u) = 1 - \Phi(u) = \frac{1}{\sqrt{2\pi}} \frac{e^{-\frac{u^2}{2}}}{u} \left(1 + O\left(\frac{1}{u^2}\right)\right), \quad u > 0. \tag{3.10}$$

Hence, for sufficiently small $\varsigma > 0$ ($\varsigma \ll \varepsilon$), we have

$$Q \approx \frac{1}{2\pi} \frac{\varsigma}{\beta} \int_0^\infty \frac{\exp\left\{-\frac{1}{2}\left(\frac{(\varepsilon h + (1-\varepsilon)s)^2}{\varsigma^2} + \frac{(s-h)^2}{\beta^2}\right)\right\}}{\varepsilon h + (1-\varepsilon)s} ds. \tag{3.11}$$

Since

$$\frac{(\varepsilon h + (1-\varepsilon)s)^2}{\varsigma^2} + \frac{(s-h)^2}{\beta^2} = \frac{(s - \varepsilon h)^2}{\varsigma^2} + \frac{h^2}{\beta^2},$$

we obtain

$$Q \approx \frac{\varsigma}{2\pi\beta} \exp\left\{-\frac{h^2}{2\beta^2}\right\} \int_0^\infty \frac{\exp\left\{-\frac{(s-h\varepsilon)^2}{2\varsigma^2}\right\}}{\varepsilon h + (1-\varepsilon)s} ds.$$

By Laplace's method [47], for sufficiently small $\varsigma > 0$ ($\varsigma \ll \varepsilon$), the last integral is asymptotic to

$$\frac{\sqrt{2\pi}}{(h\varepsilon + (1-\varepsilon)\varepsilon h)\sqrt{1/\varsigma^2}} = \frac{\sqrt{2\pi}\varsigma}{h\varepsilon(2-\varepsilon)}.$$

Hence,

$$Q \approx \frac{\varsigma}{2\pi\beta} \frac{\sqrt{2\pi}\varsigma}{h\varepsilon(2-\varepsilon)} \exp\left\{-\frac{h^2}{2\beta^2}\right\} = \frac{\beta}{\sqrt{2\pi}h} \exp\left\{-\frac{h^2}{2\beta^2}\right\}.$$

By the same reasoning the error term from (3.10) is of order

$$\exp\left\{-\frac{h^2}{2\beta^2}\right\} \times O\left(\frac{1}{\varepsilon}\left(\frac{\beta}{h}\right)^3\right),$$

which gives (3.6). □

3.3 The randomly perturbed map: random slope

Consider a process
$$Y_n = \mu(1 + \sigma r_{1,n})Y_{n-1} + \sigma r_{2,n}, \quad n \geq 1, \tag{3.12}$$

where $(r_{1,n}, r_{2,n})_{n=1}^\infty$ are IID copies of a two dimensional random vector (r_1, r_2). Here, we assume that (r_1, r_2) has bivariate normal distribution with mean vector 0 and covariance matrix $\Sigma_2 = [\sigma_{i,j}]$, where $\sigma_{i,j} = \mathrm{cov}(r_i, r_j)$, $1 \leq i, j \leq 2$. We assume that the entries $\sigma_{i,j}$ are of order 1 in a sense that they do not depend on other parameters. Recall that the probability density function of a multivariate normal random vector $(r_1, \ldots, r_d)$ with mean vector 0 and covariance matrix Σ is given by

$$\frac{1}{\sqrt{(2\pi)^d \det(\Sigma)}} \exp\left\{-\frac{1}{2}x^T \Sigma^{-1} x\right\}, \quad x = (x_1, \ldots, x_d)^T.$$

and we denote such vectors by $N(0, \Sigma)$.

For a given $h > 0$, let
$$\tau = \inf\{k \geq 1 : Y_k > h\}.$$

Theorem 3.5. *Suppose that h and $\mu \in (0,1)$ are both of order 1 and $\sigma \ll 1$ so that the following condition holds*

$$\gamma := \mu \mathbb{E}|1 + \sigma r_1| < 1. \tag{3.13}$$

Then τ is asymptotically geometric RV with parameter

$$p = \frac{\sigma}{c\sqrt{2\pi}}e^{-\frac{c^2}{2\sigma^2}}\left(1 + O(\sigma^2)\right), \tag{3.14}$$

where a positive constant c depends on h, μ, and Σ_2, but not on σ.

As before, we first establish convergence of $\{Y_n\}$ and characterize the limit. Iteration of (3.12) yields

$$\begin{aligned}
Y_n &= \mu(1 + \sigma r_{1,n})Y_{n-1} + \sigma r_{2,n} = \mu(1 + \sigma r_{1,n})\left(\mu(1 + \sigma r_{1,n-1})Y_{n-2} + \sigma r_{2,n-1}\right) + \sigma r_{2,n} \\
&= \cdots = \mu^n Y_0 \prod_{j=1}^{n}(1 + \sigma r_{1,j}) + \sigma\sum_{j=0}^{n-1}\mu^j r_{2,n-j}\prod_{\ell=n-j+1}^{n}(1 + \sigma r_{1,\ell}),
\end{aligned} \tag{3.15}$$

where as usually, $\prod_{j=k}^{m}(\,*\,) = 1$ if $k > m$.

12

Lemma 3.6.

$$Y_n \xrightarrow{d} Y \overset{d}{=} \sigma \sum_{j=0}^{\infty} \mu^j g_{2,j} \prod_{\ell=0}^{j-1}(1 + \sigma g_{1,\ell}), \ n \to \infty, \tag{3.16}$$

where $(g_{1,j}, g_{2,j})$, $j = 0, 1, 2, \ldots$ *are IID copies of two-dimensional random vector, which is equal in distribution to* (r_1, r_2).

Proof (Lemma 3.6): First, we show that Y is well-defined as the series in (3.16) converges almost surely. To see this, note that the summands

$$g_{2,j} \prod_{\ell=0}^{j-1}(1 + \sigma g_{1,\ell})$$

are martingale differences with respect to the natural filtration. By triangle inequality, independence, and (3.13),

$$\mathbb{E}\left|\sigma \sum_{j=0}^{m} \mu^j g_{2,j} \prod_{\ell=0}^{j-1}(1 + \sigma g_{1,\ell})\right| \leq \sigma \mathbb{E}|g_2| \sum_{j=0}^{m} \mu^j \mathbb{E}\left|\prod_{\ell=0}^{j-1}(1 + \sigma g_{1,\ell})\right|$$

$$= \sigma \mathbb{E}|g_2| \sum_{j=0}^{m} \mu^j \left(\mathbb{E}|1 + \sigma r_1|\right)^j = \frac{\sigma \mathbb{E}|g_2|}{1-\gamma}(1 - \gamma^{(m+1)}) \leq \frac{\sigma \mathbb{E}|g_2|}{1-\gamma}.$$

Hence, the partial sums of the right–hand side of (3.16) form an L_1–bounded martingale which converges almost surely by the martingale convergence theorem (see e.g. [42]). For every $n \geq 1$

$$\sigma \sum_{j=0}^{n-1} \mu^j r_{2,n-j} \prod_{\ell=n-j+1}^{n}(1 + \sigma r_{1,\ell}) \overset{d}{=} \sigma \sum_{j=0}^{n-1} \mu^j g_{2,j} \prod_{\ell=0}^{j-1}(1 + \sigma g_{1,\ell}).$$

Since the sequence on the right converges almost surely and the almost sure convergence implies convergence in distribution, we infer that the sequence on the left converges in distribution. To conclude that $Y_n \xrightarrow{d} Y$ it is enough to show that the first term on the right–hand side of (3.15) converges to 0 in probability. But that is clear since we have

$$\mathbb{E}\left|Y_0 \mu^n \prod_{j=1}^{n}(1 + \sigma r_{1,j})\right| = |Y_0| \mu^n \prod_{j=1}^{n} \mathbb{E}|1 + \sigma r_{1,j}| = |Y_0| \gamma^n.$$

Hence, by Markov inequality it goes to 0 in probability. $\qquad\square$

Proof (Theorem 3.5): The proof follows the lines of the proof of Theorem 3.3. The main complication in treating the present case is that we know less about the distribution of Y_n than in before. Nonetheless, we will argue that for large n

$$p_n := \frac{\mathbb{P}(\tau = n)}{\mathbb{P}(\tau \geq n)} = \mathbb{P}(\mu(1 + \sigma r_{1,n})Y_{n-1} + \sigma r_{2,n} > h|Y_{n-1} \leq h) \tag{3.17}$$

is approximately constant. For this, we rewrite the right hand side of (3.17) as

$$\frac{\mathbb{P}(\mu(1+\sigma r_{1,n})Y_{n-1}+\sigma r_{2,n}>h, Y_{n-1}\leq h)}{\mathbb{P}(Y_{n-1}\leq h)},$$

and since the denominator converges to $\mathbb{P}(Y\leq h)$ we focus on the numerator. Let (r_1, r_2) be a generic vector distributed like $(r_{1,n}, r_{2,n})$ and independent of Y. Since for every $n\geq 1$, $(r_{1,n}, r_{2,n})$ is independent of Y_{n-1}, as $n\to\infty$ we have

$$(r_{1,n}, r_{2,n}, Y_{n-1}) \xrightarrow{d} (r_1, r_2, Y).$$

Thus,

$$\mathbb{P}(\mu(1+\sigma r_1)Y_{n-1}+\sigma r_2 > h, Y_{n-1}\leq h) \longrightarrow \mathbb{P}(\mu(1+\sigma r_1)Y+\sigma r_2 > h, Y\leq h),$$

which establishes the existence of $p = \lim_{n\to\infty} p_n$.

To estimate p, we first recall that (r_1, r_2) is bivariate normal if and only if every linear combination of r_1 and r_2 is a normal RV. Hence, conditionally on $Y = y$, $\sigma(\mu y r_1 + r_2)$ is $N(0, \sigma^2 \sigma_y^2)$ RV, where

$$\sigma_y^2 = \sigma_{22}^2 + \mu^2 y^2 \sigma_{11}^2 + 2\mu y \sigma_{12}. \tag{3.18}$$

Therefore,

$$\mathbb{P}(\mu(1+\sigma r_1)Y+\sigma r_2 > h, \ Y\leq h) = \mathbb{P}(\sigma(\mu Y r_1 + r_2) > h - \mu Y, Y\leq h)$$

$$= \int_{-\infty}^{h} \mathbb{P}(Z > \frac{h-\mu y}{\sigma\sigma_y}) dF_Y(y) = \int_{-\infty}^{h} \left(1 - \Phi\left(\frac{h-\mu y}{\sigma\sigma_y}\right)\right) dF_Y(y)$$

$$= \left(1 - \Phi\left(\frac{h-\mu y_0}{\sigma\sigma_{y_0}}\right)\right) \mathbb{P}(Y\leq h),$$

where $-\infty < y_0 < h$ by the mean value theorem. Hence,

$$p = \frac{\mathbb{P}(\mu(1+\sigma r_1)Y+\sigma r_2 > h, \ Y\leq h)}{\mathbb{P}(Y\leq h)} = 1 - \Phi\left(\frac{h-\mu y_0}{\sigma\sigma_{y_0}}\right).$$

Let $c := c(y_0)$ where

$$c(x) = c_{h,\mu,\Sigma_2}(x) := \frac{h-\mu x}{\sigma_x} = \frac{h-\mu x}{\sqrt{\mu^2\sigma_{11}^2 x^2 + 2\mu\sigma_{12}x + \sigma_{22}^2}}.$$

Then, by (3.10)

$$p = 1 - \Phi\left(\frac{c}{\sigma}\right) = \frac{\sigma}{c\sqrt{2\pi}} e^{-\frac{c^2}{2\sigma^2}} \left(1 + O\left(\frac{\sigma^2}{c^2}\right)\right).$$

Furthermore, by elementary analysis we see that:

- $c(x)$ is increasing on $x \in (-\infty, x^*)$ and decreasing on $x \in (x^*, \infty)$, where

$$x^* = -\frac{\sigma_{11}^2 + h\sigma_{12}}{\mu(h\sigma_{22}^2 + \sigma_{12})},$$

14

- $c(-\infty) = \sigma_{11}^{-1}$, $c(h) = \dfrac{(1-\mu)h}{((\mu h \sigma_{11})^2 + 2\mu\sigma_{12}h + \sigma_{22})^{1/2}} = \dfrac{(1-\mu)h}{((\mu h \sigma_{11} + \sigma_{22})^2 - 2\mu h(\sigma_{11}\sigma_{22} - \sigma_{12}))^{1/2}}$, and $c(x^*)$ is given by a quite unwieldy expression that depends on h and Σ_2 but not on μ.

In particular, c is bounded away from 0 and ∞ provided μ and h are positive and $\mu < 1$. This proves (3.14). $\square$

3.4 A two-dimensional randomly perturbed map

In this subsection we consider the following two dimensional model:

$$\xi_{n+1} = \mu\xi_n(1 + \sigma r_{1,n+1}) + \sigma r_{2,n+1}, \tag{3.19}$$

$$\eta_{n+1} = \lambda\eta_n + \epsilon\sigma r_{3,n+1} + \epsilon a_2\xi_n. \tag{3.20}$$

where $(r_{1,n}, r_{2,n}, r_{3,n})$, $n \geq 1$, is a sequence of IID copies of (r_1, r_2, r_3) which, as follows form a discussion at the beginning of Section 4.4 is assumed to be a trivariate normal random vector $N(0, \Sigma_3)$, with $\Sigma_3 = [\sigma_{i,j}]$, $1 \leq i, j \leq 3$, where $\sigma_{i,j} = \mathrm{cov}(r_i, r_j)$ do not depend on any parameters in (4.44) and (4.45). For positive $h_1, h_2 = O(1)$, we define

$$\tau_\xi = \inf_{k \geq 1}\{\xi_k > h_1\}, \qquad \tau_\eta = \inf_{k \geq 1}\{\eta_k > h_2\}.$$

We are interested in $\tau = \min\{\tau_\xi, \tau_\eta\}$. We know the distribution of τ_ξ from Theorem 3.5. As we will show below, under the suitable conditions the distribution of τ is again asymptotically geometric. Moreover, if $\epsilon > 0$ is small then τ_η has practically no effect on the distribution of τ.

In order to be more precise, let us define

$$A_n = \begin{bmatrix} \mu(1 + \sigma r_{1,n}) & 0 \\ \epsilon a_2 & \lambda \end{bmatrix}, \quad G_n = \begin{bmatrix} r_{2,n} \\ \epsilon r_{3,n} \end{bmatrix}, \quad \text{and} \quad \Theta_n = \begin{bmatrix} \xi_n \\ \eta_n \end{bmatrix}. \tag{3.21}$$

Then, (3.19) and (3.20) are described by

$$\Theta_{n+1} = A_{n+1}\Theta_n + \sigma G_{n+1}, \quad n \geq 1. \tag{3.22}$$

Theorem 3.7. *Let $\mu, \sigma, \epsilon \in (0, 1)$ be such that μ is of order 1 and $\sigma \ll 1$ so that condition (3.13) holds. Assume $\epsilon \ll 1$ and set $\lambda = 1 - \epsilon$. Suppose further that h_1 and h_2 are of order 1. Then τ is approximately geometric RV with parameter p satisfying*

$$p \approx \frac{\sigma}{c\sqrt{2\pi}}e^{-\frac{c^2}{2\sigma^2}}, \tag{3.23}$$

and where the constant c depends on h_1, μ, and Σ_3 but not on σ.

The following lemma shows that $\{\Theta_n\}$ converges in distribution and describes the limit.

Lemma 3.8.

$$\Theta_n \xrightarrow{d} X \stackrel{d}{=} \sigma \sum_{k=1}^{\infty} \left(\prod_{j=1}^{k-1} A_j \right) G_k, \ n \to \infty, \tag{3.24}$$

where A_n and $G_n, n = 1, 2, dots$ are defined in (3.21). Furthermore, this random vector X satisfies the distributional equation

$$X \stackrel{d}{=} AX + \sigma G, \tag{3.25}$$

where

$$A = \begin{bmatrix} \mu(1 + \sigma r_1) & 0 \\ \epsilon a_2 & \lambda \end{bmatrix} \quad \text{and} \quad G = \begin{bmatrix} r_2 \\ \epsilon r_3 \end{bmatrix}, \tag{3.26}$$

(r_1, r_2, r_3) is $N(0, \Sigma_3)$ be generic copies of A_n and G_n, and, X on the right hand side of (3.25) is independent of (A, G).

Proof (Lemma 3.8): Note first that each of the sequences (A_n) and (G_n) consists of IID random elements. Let (r_1, r_2, r_3) is $N(0, \Sigma_3)$ be generic copies of A_n and G_n. By iterating (3.22), we obtain

$$\Theta_n = A_n(A_{n-1}\Theta_{n-2} + \sigma G_{n-1}) + \sigma G_n = \cdots = \left(\prod_{k=0}^{n-1} A_{n-k} \right) \Theta_0 + \sigma \sum_{k=1}^{n} \left(\prod_{j=0}^{n-k-1} A_{n-j} \right) G_k,$$

where, as usually, the product is set to be 1 if its index range is empty. We have

$$\prod_{k=0}^{n-1} A_{n-k} = \begin{bmatrix} \mu^n \prod_{k=1}^{n}(1 + \sigma r_{1,k}) & 0 \\ T_n & \lambda^n \end{bmatrix},$$

where

$$T_n = \epsilon a_2 \sum_{j=1}^{n} \lambda^{n-j} \prod_{k=1}^{j-1} (\mu(1 + \sigma r_{1,k})).$$

Set $\delta = \max\{\lambda, \mu\mathbb{E}|1 + \sigma r_1|\}$ and note that by (3.13) $\delta < 1$. By triangle inequality and independence of $r_{1,k}$'s

$$\mathbb{E}|T_n| \leq \epsilon a_2 \sum_{j=1}^{n} \lambda^{n-j} \mathbb{E} \left| \prod_{k=1}^{j-1} (\mu(1 + \sigma r_{1,k})) \right| = \epsilon a_2 \sum_{j=1}^{n} \lambda^{n-j} \left(\mu\mathbb{E}|1 + \sigma r_1| \right)^{j-1} \leq \epsilon a_2 n \delta^{n-1}.$$

Similarly,

$$\mu^n \mathbb{E} \left| \prod_{k=1}^{n} (1 + \sigma r_{1,k}) \right| = (\mu\mathbb{E}|1 + \sigma r_1|)^n \leq \delta^n.$$

It follows that both components of $\left(\prod_{k=0}^{n-1} A_{n-k} \right) \Theta_0$ converge to 0 in probability and thus, this term is negligible.

Since the sequences (A_n) and (G_n) are IID, for every $n \geq 1$ we have

$$\sum_{k=1}^{n} \left(\prod_{j=0}^{n-k-1} A_{n-j} \right) G_k \stackrel{d}{=} \sum_{k=1}^{n} \left(\prod_{j=1}^{k-1} A_j \right) G_k.$$

16

By the same argument as above we verify that both components of the sequence of partial sums on the right hand side are Cauchy in L_1. Hence, the components of the series

$$\sum_{k=1}^{\infty} \left(\prod_{j=1}^{k-1} A_j \right) G_k,$$

converge in probability (and thus, in distribution). Therefore, the sequence (Θ_n) defined by (3.22) converges in distribution to a random vector X defined in (3.24). Furthermore, X satisfies the distributional equation (3.25). $\qquad\square$

Proof (Theorem 3.7): For $h = (h_1, h_2)$ set $B_h := (-\infty, h_1] \times (-\infty, h_2]$. Then

$$\{\tau = n\} = \{\Theta_j \in B_h,\ j < n,\ \Theta_n \notin B_h\},$$

so that

$$\begin{aligned}
\mathbb{P}(\tau = n) &= \mathbb{P}(\Theta_n \notin B_h | \Theta_j \in B_h,\ j < n)\mathbb{P}(\Theta_j \in B_h,\ j < n) \\
&= \mathbb{P}(A_n\Theta_{n-1} + \sigma G_n \notin B_h | \Theta_{n-1} \in B_h)\mathbb{P}(\tau \geq n).
\end{aligned}$$

Since Θ_n converge in distribution to X we have

$$p_n := \mathbb{P}(A_n\Theta_{n-1} + \sigma G_n \notin B_h | \Theta_{n-1} \in B_h) = \frac{\mathbb{P}(A_n\Theta_{n-1} + \sigma G_n \notin B_h, \Theta_{n-1} \in B_h)}{\mathbb{P}(\Theta_{n-1} \in B_h)}$$

$$\longrightarrow p := \frac{\mathbb{P}(AX + \sigma G \notin B_h, X \in B_h)}{\mathbb{P}(X \in B_h)}, \quad \text{as} \quad n \to \infty. \tag{3.27}$$

It follows from (3.24) that X is symmetric, so since both h_1 and h_2 are positive the denominator is at least $1/2$ and does not affect the asymptotics.

To handle the numerator, using (3.26), denoting the components of X by X_1 and X_2, and using the notation adopted in (3.18) we see that it is equal to

$$\begin{aligned}
&\mathbb{P}((\mu(1 + \sigma r_1)X_1 + \sigma r_2, \epsilon a_2 X_1 + \lambda X_2 + \epsilon \sigma r_3) \notin B_h, (X_1, X_2) \in B_h) \\
&= \mathbb{P}(\mu(1 + \sigma r_1)X_1 + \sigma r_2 > h_1, (X_1, X_2) \in B_h) \\
&\quad + \mathbb{P}(\epsilon a_2 X_1 + \lambda X_2 + \epsilon \sigma r_3 > h_2, (X_1, X_2) \in B_h) \\
&\quad\quad - \mathbb{P}(\mu(1 + \sigma r_1)X_1 + \sigma r_2 > h_1, \epsilon a_2 X_1 + \lambda X_2 + \epsilon \sigma r_3 > h_2, (X_1, X_2) \in B_h) \\
&= \mathbb{P}\left(\frac{\mu X_1 r_1 + r_2}{\sigma_{X_1}} > \frac{h_1 - \mu X_1}{\sigma \sigma_{X_1}}, (X_1, X_2) \in B_h \right) \\
&\quad + \mathbb{P}\left(r_3 > \frac{h_2 - \epsilon a_2 X_1 - \lambda X_2}{\epsilon \sigma}, (X_1, X_2) \in B_h \right) \\
&\quad\quad - \mathbb{P}\left(\frac{\mu X_1 r_1 + r_2}{\sigma_{X_1}} > \frac{h_1 - \mu X_1}{\sigma \sigma_{X_1}}, r_3 > \frac{h_2 - \epsilon a_2 X_1 - \lambda X_2}{\epsilon \sigma}, (X_1, X_2) \in B_h \right). \tag{3.28}
\end{aligned}$$

Conditionally on $(X_1, X_2) = (x_1, x_2)$,

$$Z_1 := \frac{\mu x_1 r_1 + r_2}{\sigma_{x_1}}, \quad \text{and} \quad Z_2 := \frac{r_3}{\sigma_{33}}$$

17

are $N(0,1)$ RVs. Hence by letting $F_X(x_1, x_2)$ denote the distribution function of (X_1, X_2), we see that the first of the last three probabilities is

$$\int_{-\infty}^{h_2} \int_{-\infty}^{h_1} \left(1 - \Phi\left(\frac{h_1 - \mu x_1}{\sigma \sigma_{x_1}} \right) \right) dF_X(x_1, x_2), \tag{3.29}$$

Likewise, for the second of these probabilities we get

$$\int_{-\infty}^{h_2} \int_{-\infty}^{h_1} \left(1 - \Phi\left(\frac{h_2 - \epsilon a_2 x_1 - \lambda x_2}{\epsilon \sigma \sigma_{33}} \right) \right) dF_X(x_1, x_2). \tag{3.30}$$

We now note that if ϵ is of a smaller order than all other parameters (except possibly σ) then (3.10) implies that (3.30) (and hence also (3.28)) are negligible when compared to (3.29). To analyze the behavior of (3.29) as a function of its parameters note that by the mean value theorem the quantity in (3.29) is equal to

$$\left(1 - \Phi\left(\frac{h_1 - \mu x_0}{\sigma \sigma_{x_0}} \right) \right) \int_{-\infty}^{h_2} \int_{-\infty}^{h_1} dF_X(x_1, x_2) = \left(1 - \Phi\left(\frac{h_1 - \mu x_0}{\sigma \sigma_{x_0}} \right) \right) \mathbb{P}(X \in B_h),$$

for some $-\infty < x_0 < h$. Substituting this into (3.27) (and neglecting the terms that depend on ϵ) we see that

$$p = \frac{\mathbb{P}(AX + \sigma G \notin B_h, X \in B_h)}{\mathbb{P}(X \in B_h)} \sim 1 - \Phi\left(\frac{h_1 - \mu x_0}{\sigma \sigma_{x_0}} \right).$$

If both $0 < \mu < 1$ and h_1 are of order 1 we are in the same situation as with (3.14). This shows (3.23). $\quad\square$

3.5 Diffusive escape

The exit problems for the stochastic difference equations analyzed in the previous subsections all feature the geometric escape mechanism. In the simplest case when the evolution is given by Equation (3.4), the geometric distribution characterizes the statistics of the times of exit of the trajectories of (3.4) from a certain neighborhood of the attracting fixed point. In this subsection, we study another important in applications statistical regime associated with the exit problem for (3.4), the diffusive regime. The role of the diffusive regime in characterizing the statistics of the exit times for the trajectories of (3.4) is twofold. First, the geometric distribution approximates the distribution of the exit times only for sufficiently large times, i.e. for large n. In this subsection, we show that in the intermediate range of n, i.e. when n is neither too large nor too small, Y_n's are approximated by the sums of the IID RVs and, therefore, the level exceedance times are distributed as those for random walks. We refer to this situation as the diffusive regime. Second, we recall that to justify the geometric distribution in the proof of Theorem 3.3, we implicitly assumed that the rate of attraction of the fixed point is stronger than the noise intensity. Specifically, it is easy to see from the proof of Theorem 3.3 that ς is required to be $o(\epsilon)$, $\epsilon = 1 - \lambda$. The analysis in this subsection does not use this assumption. We show that when the noise is stronger than the attraction of the fixed point (albeit both are sufficiently small), the mechanism of escape of the trajectories from the basin of attraction of the fixed point changes from the geometric to diffusive. Therefore, we conclude this section by pointing out to some features intrinsic to the diffusive escape. Specifically, we consider (3.4), for which as before, we define
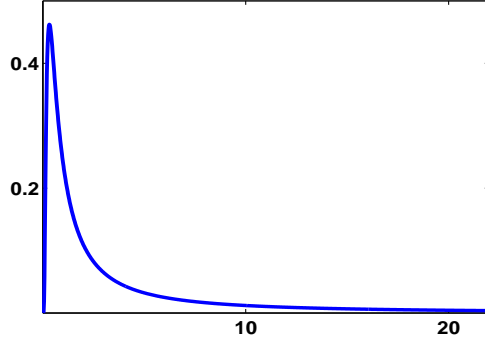
$$\tau = \inf\{k \geq 1 : Y_k > h\}, \tag{3.31}$$

18

Figure 5: Probability density function corresponding to the distribution $\Psi_a(y), a = 1$. With a suitable $a > 0$, $\Psi_a(y)$ approximates the distribution of the exit times in the diffusive escape.

for given $h > 0$. In contrast to the case considered in Section 3.2, here we assume

$$\varepsilon = O(\varsigma^\alpha), \quad \alpha > 0. \tag{3.32}$$

In Theorem 3.9 below, we show that in the present situation in the intermediate range of n, $Y_n's$ behave as sums of IID normal RVs. The behavior of the latter is well-known (cf, Lemma 3.11).

Recall that $\Phi(x)$ stands for the distribution function of an $N(0, 1)$ RV and denote

$$\Psi_a(x) = 2\left(1 - \Phi\left(\frac{a}{\sqrt{x}}\right)\right), \quad a > 0. \tag{3.33}$$

Note that $\Psi_a(x)$ is a probability distribution function on $\mathbb{R}^+$ (see Fig. 5).

Theorem 3.9. *Let the evolution of Y_n, $n = 0, 1, 2, \ldots$ be given by (3.4). Suppose that $\lambda = 1 - \varepsilon$ with $\varepsilon = O\left(\varsigma^\alpha\right)$, $\alpha > 0$. Then for arbitrary positive β_1 and β_2 such that $\beta_1 + \beta_2 < 2\alpha/3$, for sufficiently small $\varsigma > 0$,*

$$\mathbb{P}(\tau \le n) = \Psi_a(n)\left(1 + o(1)\right), \quad a = \frac{h}{\varsigma}, \tag{3.34}$$

in the range $\varsigma^{-\beta_1} \ll n \ll \varsigma^{\frac{-2\alpha}{3} + \beta_2}$.

Remark 3.10. Since $\beta_{1,2} > 0$ are arbitrary, $\Psi_a(n)$ practically approximates $\mathbb{P}(\tau \le n)$ in the range $1 \ll n \ll \varepsilon^{-2/3}$.

We will need the following auxiliary lemma [11, Theorem 2.2, Chapter III]. It may be viewed as a quantified version of a reflection principle for random walk (see, e.g., [42, Sec. 5.3, 5.4]).

Lemma 3.11. *Let $X_1, X_2, \ldots$ be a sequence of independent, symmetric RVs and set*

$$S_k = \sum_{j=1}^{k} X_j, \quad and \quad S_k^* = \max_{1 \le j \le k} S_j, \quad j \ge 1.$$

19

Then for any $t, u > 0$ the following inequalities hold:

$$2\mathbb{P}(S_n \geq t + 2u) - 2\sum_{k=1}^{n}\mathbb{P}(X_k \geq u) \leq \mathbb{P}(S_n^* \geq t) \leq 2\mathbb{P}(S_n \geq t). \tag{3.35}$$

Remark 3.12. As was noticed by S. Kwapień a bit stronger version of the first inequality in (3.35) follows from a slight modification of the proof of Proposition 1.3.1 in [30].

Proof (Theorem 3.9): Without loss of generality, we assume that $Y_0 = 0$ (otherwise, apply the same argument to $Y_k - Y_0$). Note that the distributions of τ and Y_k^* are linked by the following relation

$$\mathbb{P}(\tau \leq n) = \mathbb{P}(Y_n^* \geq h).$$

Unwinding (3.4) and using $Y_0 = 0$ gives

$$Y_k = \varsigma(\lambda^{k-1}r_1 + \lambda^{k-2}r_2 + \cdots + \lambda r_{k-1} + r_k),$$

which we write as $S_k + W_k$, where

$$S_k := \varsigma\sum_{j=1}^{k}r_j, \qquad W_k := \varsigma\sum_{j=1}^{k-1}r_j(\lambda^{k-j} - 1). \tag{3.36}$$

We will first show that the main contribution to Y_n^* is from the S_n^*. First, by subadditivity of maxima, for any $0 < h_1 < h$,

$$\begin{aligned}\mathbb{P}(Y_n^* \geq h) \leq \mathbb{P}(S_n^* + W_n^* \geq h) &\leq \mathbb{P}(S_n^* \geq h - h_1) + \mathbb{P}(W_n^* \geq h_1) \\ &\leq \mathbb{P}(S_n^* \leq h - h_1) + \mathbb{P}\left(|W_n|^* \geq h_1\right).\end{aligned} \tag{3.37}$$

Further, $Y_k \geq S_k - |W_k|$ so that

$$\mathbb{P}(S_n^* \geq h + h_1) \leq \mathbb{P}(S_n^* \geq h + h_1, |W_n|^* < h_1) + \mathbb{P}(|W_n|^* \geq h_1) \leq \mathbb{P}(Y_n^* \geq h) + \mathbb{P}(|W_n|^* \geq h_1),$$

which, when combined with (3.37) means that

$$\mathbb{P}(S_n^* \geq h + h_1) - \mathbb{P}(|W_n|^* \geq h_1) \leq \mathbb{P}(Y_n^* \geq h) \leq \mathbb{P}(S_n^* \geq h - h_1) + \mathbb{P}(|W_n|^* \geq h_1). \tag{3.38}$$

First, we estimate $\mathbb{P}(|W_n|^* \geq h_1)$ in (3.38). To this end, we use $1 - \lambda^j = 1 - (1 - \varepsilon)^j \leq j\varepsilon$ to obtain

$$\operatorname{var}(W_n) = \varsigma^2\sum_{j=1}^{n-1}(1 - \lambda^j)^2 \leq \varsigma^2\varepsilon^2\frac{n^3}{3} = \varsigma^2 n\frac{\varepsilon^2 n^2}{3}.$$

Consequently, by (3.35) and (3.36), we have

$$\begin{aligned}\mathbb{P}(|W_n|^* \geq h_1) &\leq 2\mathbb{P}(|W_n| \geq h_1) \leq 4\mathbb{P}(W_n \geq h_1) = 4\mathbb{P}\left(Z \geq \frac{h_1}{\sqrt{\operatorname{var}(W_n)}}\right) \\ &\leq 4\mathbb{P}\left(Z \geq \frac{h_1}{\varsigma\sqrt{n}} \cdot \frac{\sqrt{3}}{\varepsilon n}\right).\end{aligned}$$

20

Next, we turn to estimating the probabilities involving S_n^* in (3.38). By the second inequality in (3.35), for every $u > 0$, we have

$$\mathbb{P}(S_n^* \geq h - h_1) \leq 2\mathbb{P}(S_n \geq h - h_1) = 2\mathbb{P}\left(Z \geq \frac{h - h_1}{\varsigma\sqrt{n}}\right), \tag{3.39}$$

while the first one yields

$$\begin{aligned}
\mathbb{P}(S_n^* \geq h + h_1) &\geq& 2\mathbb{P}\left(S_n \geq h + h_1 + 2u\right) - 2\sum_{k=1}^{n}\mathbb{P}(\varsigma r_k \geq u) \\
&=& 2\mathbb{P}\left(Z \geq \frac{h + h_1 + 2u}{\varsigma\sqrt{n}}\right) - 2n\mathbb{P}\left(Z \geq \frac{u}{\varsigma}\right).
\end{aligned} \tag{3.40}$$

The combination of (3.38), (3.39), and (3.40) yields

$$\mathbb{P}(Y_n^* \geq h) \geq 2\mathbb{P}\left(Z \geq \frac{h + h_1 + 2u}{\varsigma\sqrt{n}}\right) - 2n\mathbb{P}\left(Z \geq \frac{u}{\varsigma}\right) - 4\mathbb{P}\left(Z \geq \frac{h_1}{\varsigma\sqrt{n}} \cdot \frac{\sqrt{3}}{\varepsilon n}\right), \tag{3.41}$$

$$\mathbb{P}(Y_n^* \geq h) \leq 2\mathbb{P}\left(Z \geq \frac{h - h_1}{\varsigma\sqrt{n}}\right) + 4\mathbb{P}\left(Z \geq \frac{h_1}{\varsigma\sqrt{n}} \cdot \frac{\sqrt{3}}{\varepsilon n}\right) \tag{3.42}$$

To complete the proof, we need to chose h_1 and u such that

$$\frac{h_1}{\varsigma\sqrt{n}} = o(1), \quad \frac{u}{\varsigma\sqrt{n}} = o(1), \quad \frac{\varsigma}{u} = o(1), \quad \text{and} \quad h_1^{-1}\varsigma\varepsilon n^{3/2} = o(1). \tag{3.43}$$

It is straightforward to verify that relations in (3.43) hold with $h_1 = \varsigma^{1 + \frac{3\beta}{2}}$ and $u = \varsigma^{1 - \frac{\beta_1}{2}}$, $\beta_{1,2} > 0$, $\beta_1 + \beta_2 < 2\alpha/3$, and n as in (3.34). $\qquad\square$

4   The Poincare map

In the present section, we consider the type I model, i.e. the randomly perturbed system with the stochastic forcing acting via the fast subsystem (see (2.9) and (2.10)). In the active phase of bursting (when the system undergoes spiking), the trajectory of the randomly perturbed system remains in the vicinity of the cylinder foliated by the periodic orbits of the fast subsystems, (see Fig. 6a). The time that the trajectory spends near L determines the duration of the active phase. The goal of this section is to describe the slow dynamics near L. In particular, we will estimate the distribution of the number of spikes in one burst. To this end, we introduce a transverse to L crossection Σ (see Fig. 6a) and construct the first return map. Specifically, we estimate the change in the state of the system after one cycle of rotation of the trajectory around L. The construction of the first return map for (2.9) and (2.10) is done in analogy to that for the deterministic models of bursting (see [34, 31]). However, the treatment of the randomly perturbed system requires certain modifications. First, we have to resolve the ambiguity in the notion of the first return time. The latter is due to the fact that generically a trajectory of the randomly perturbed system makes multiple crossings

with Σ during each cycle around L. We refer the reader to the comments following Theorem 2.3 in [19] for an explicit example illustrating this effect. For the randomly perturbed system, we define the time of the first return so that it approaches the first-return time of the underlying deterministic system in the limit of vanishing random perturbation. The definition of the first return time motivates the definition of the Poincare map (see Definition 4.1). In Sections 4.1 and 4.2, we use asymptotic expansions to construct the linear approximation for the Poincare map of the fast subsystem. Here, we use an obvious observation that on finite time intervals and for sufficiently small $\epsilon > 0$, the slow variable typically remains in an $O(\epsilon)$ neighborhood of its initial value. Therefore, for finite times the Poincare map of the fast subsystem captures the dynamics of the full system. Since we are interested in long term behavior of the system, to complete the description of the first return map we also need to track the (small) changes in the slow variable after each cycle of oscillations. This is done in Section 4.3, where we derive a $1D$ map for the slow variable. The combination of the $1D$ Poincare map for the fast subsystem and that for the slow variable provides the first return map for the full problem (2.9) and (2.10). The linear approximation of the $2D$ map is used in Section 4.4 to estimate the distribution of the number of spikes in one burst for the type I model. Effectively, the problem is reduced to the exit problem for a $1D$ linear randomly perturbed map. For the latter problem, we have already developed necessary analytical tools in Section 3. Finally, in Section 4.5, we comment on the straightforward modifications necessary to extend the analysis of this section to cover type II models.

4.1 Preliminary transformations

Recall that Σ stands for the transverse section located as shown schematically in Fig. 6a. Let $y_0 < y_{bp}$ be outside an $O(\sigma)$ neighborhood of y_{bp}, and $x_0 = \left(x_0^1, x_0^2\right)^T \in \Sigma$ be from an $O(\sigma)$ neighborhood of L. Consider an initial value problem for (2.9) and (2.10) with initial data (x_0, y_0). By standard results from the asymptotic theory for randomly perturbed systems [19], we have the following estimate

$$y_t = y_0 + O(\epsilon), \tag{4.1}$$

valid on a finite interval of time $t \in [0, \bar{t}]$. Here and below, for a small parameter $\epsilon > 0$, the symbols $O(\epsilon)$ and $o(\epsilon)$ in the asymptotic expansions of the random functions mean that the corresponding relations hold almost surely (a.s.). Specifically, $\psi_t(\epsilon) = O(\epsilon)$ for $t \in [t_1, t_2]$ means that there exists $\epsilon_0 > 0$ such that

$$\sup_{\substack{t \in [t_1, t_2] \\ \epsilon \in [0, \epsilon_0]}} \left| \epsilon^{-1} \psi_t(\epsilon) \right| < \infty \quad \text{a.s..}$$

In a similar fashion, we interpret $\psi_t(\epsilon) = o(\epsilon)$ when $\psi_t(\epsilon)$ is a random function.

By plugging in (4.1) into (2.9), we obtain the following SODE

$$dx_t = f(x_t)\,dt + \sigma p(x_t)dw_t + O(\epsilon), \tag{4.2}$$

where $f(x) := f(x, y_0)$, $p(x) := p(x, y_0)$, and y_0 is fixed. Equation (4.2) with $\epsilon = \sigma = 0$ has an exponentially orbitally stable periodic solution $x = \phi(t, y_0)$ of period $\mathcal{T}(y_0)$:

$$L(y_0) = \{x = \phi(\theta, y_0) : \ \theta \in [0, \mathcal{T}(y_0))\} \qquad \text{(cf. (2.2)).}$$

22

To simplify the notation, throughout the analysis of the fast subsystem, we will omit to indicate the dependence on y_0 when refer to L, ϕ, and $\mathcal{T}$. At each point $x = \phi(\theta) \in L$, we define vectors

$$\tau(\theta) = \left(f^1(x), f^2(x)\right)^T \quad \text{and} \quad \nu(\theta) = Jf(x), \;\; \text{where} \;\; J = \begin{pmatrix} 0 & -1 \\ 1 & 0 \end{pmatrix}, \tag{4.3}$$

pointing in the tangential and normal directions, respectively. To study the trajectories of (4.2) in a small neighborhood of L, it is convenient to rewrite (4.2) in normal coordinates (θ, ξ) [23]:

$$x = \phi(\theta) + \xi \nu(\theta), \quad \theta \in [0, \mathcal{T}). \tag{4.4}$$

Lemma 4.1. *For sufficiently small $\delta > 0$ Equation (4.4) defines a smooth change of coordinates in*

$$B_\delta = \{x = \phi(\theta) + \xi \nu(\theta) : \; |\xi| < \delta, \; \theta \in [0, \mathcal{T})\}. \tag{4.5}$$

In new coordinates, (4.2) has the following form:

$$\begin{align}
d\theta_t &= (1 + b_1(\theta_t)\xi_t)dt + \sigma h_1(\theta_t, \xi_t)\left(1 + b_2(\theta_t)\xi_t\right)dw_t + O(\epsilon, \delta^2, \sigma^2), \tag{4.6} \\
d\xi_t &= a(\theta_t)\xi_t dt + \sigma h_2(\theta_t, \xi_t)dw_t + O(\epsilon, \delta^2, \sigma^2), \tag{4.7}
\end{align}$$

where smooth functions $a(\theta), b_1(\theta),$ and $b_2(\theta)$ are $\mathcal{T}-$periodic and

$$0 < \mu := \exp\left(\int_0^{\mathcal{T}} a(\theta)d\theta\right) = \exp\left(\int_0^{\mathcal{T}} \mathrm{div}f\left(\phi(\theta)\right)\right) < 1, \tag{4.8}$$

$$h_1(\theta, \xi) = \frac{<p, \tau>}{<\tau, \tau>} = \frac{p^1 f^1 + p^2 f^2}{|f|^2}, \;\; h_2(\theta, \xi) = \frac{<p, \nu>}{<\tau, \tau>} = \frac{p^2 f^1 - p^1 f^2}{|f|^2}. \tag{4.9}$$

Proof : The proof of the lemma follows the lines of the proof of Theorem VI.1.2 in [23]. Let $z = (z^1, z^2)^T := (\theta, \xi)^T$ and denote the transformation in (4.4) by

$$x = v(z), \; z \in B_\delta. \tag{4.10}$$

Note

$$|Dv(\theta, 0)| = \begin{vmatrix} \phi^{1'}(\theta) & -f^2\left(\phi(\theta)\right) \\ \phi^{2'}(\theta) & f^1\left(\phi(\theta)\right) \end{vmatrix} = |f\left(\phi(\theta)\right)|^2 \neq 0, \; \theta \in [0, \mathcal{T}).$$

Therefore, for sufficiently small $\delta > 0$, (4.10) defines a smooth invertible transformation in B_δ. Denote the inverse of v by $z = u(x)$, $x \in v(B_\delta)$ and note that

$$[Du(x)]^{-1} = Dv(z), \; x \in v(B_\delta). \tag{4.11}$$

By Itô's formula, we have

$$dz_t = Du(x_t)dx_t + O(\sigma^2)dt \tag{4.12}$$

and, therefore,

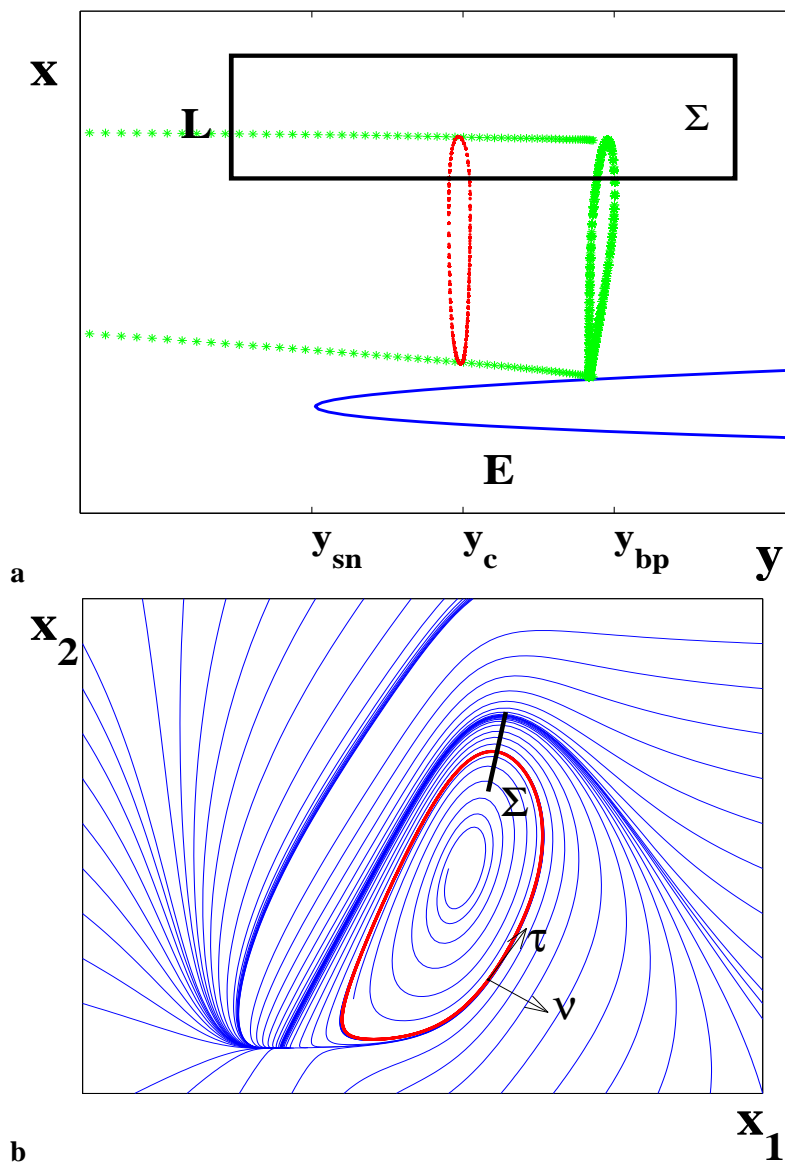$$Dv(z_t)dz_t = dx_t + O(\sigma^2)dt. \tag{4.13}$$

23

Figure 6: (a) Crossection Σ is used in the construction of the first return map. (b) The phase plane of the fast subsystem (2.1) for $y \in (y_{sn}, y_{bp})$.

By recalling that $z = (\theta, \xi)$ and after plugging in (4.2) into (4.13), we obtain

$$\left[\frac{d\phi(\theta_t)}{d\theta} + \frac{d\nu(\theta_t)}{d\theta}\xi_t\right] d\theta_t + \nu(\theta_t)d\xi_t = (f(\phi(\theta_t)) + Df(\phi(\theta_t))\nu(\theta_t)\xi_t + Q(\theta_t, \xi_t)) dt$$
$$+ \sigma p dw_t + O(\epsilon, \sigma^2), \tag{4.14}$$

where

$$Q(\theta, \xi) = f(\phi(\theta) + \xi\nu(\theta)) - f(\phi(\theta)) - Df(\phi(\theta))\nu(\theta)\xi = O(\xi^2), \quad |\xi| < \delta.$$

Note that

$$\frac{d\phi(\theta)}{d\theta} = f(\phi(\theta)) = \tau(\theta), \quad \tau^T(\theta)\tau(\theta) = \nu(\theta)^T\nu(\theta) = |f(\phi(\theta))|^2, \tag{4.15}$$

$$\frac{d\nu(\theta)}{d\theta} = \frac{d}{d\theta}Jf(\phi(\theta)) = JDf(\phi(\theta))f(\phi(\theta)). \tag{4.16}$$

Taking into account (4.15) and (4.16), we project (4.14) onto the subspace spanned by $\tau(\theta_t)$ and after some algebra obtain:

$$\dot{\theta}_t = 1 + \frac{f^T Q + f^T [DfJ - JDf] f\xi_t + \sigma f^T p\dot{w}_t + O(\epsilon)}{f^T f + f^T JDff\xi_t}. \tag{4.17}$$

Here and for the rest of the proof, for brevity we use the following notation:

$$f := f(\phi(\theta_t)), \quad Q := Q(\theta_t, \xi_t), \quad \text{and} \quad \nu := \nu(\theta_t).$$

Equation (4.17) can be rewritten as (4.6) with

$$b_1(\theta_t) = \frac{1}{|f|^2} f^T [DfJ - JDf] f,$$

$$b_2(\theta_t) = \frac{1}{|f|^2} f^T JDff.$$

Similarly, by projecting (4.14) onto the subspace spanned by $\nu(\theta)$ and using (4.15) and (4.14), we derive

$$\dot{\xi}_t = a(\theta_t)\xi_t + \sigma h_2(\theta_t)\dot{w}_t + O(\delta^2),$$

where

$$a(\theta_t) = \frac{1}{|\nu|^2}\nu^T \left[Df\nu + \frac{d\nu}{d\theta}\right] - \frac{2\nu^T}{|\nu|^2}\frac{d\nu}{d\theta}.$$

The expression in the square brackets can be simplified as follows:

$$\nu^T \left[Df\nu + \frac{d\nu}{d\theta}\right] = f^T \left[J^T DfJ + Df\right] = \operatorname{div} f(\phi(\theta)) |f|^2.$$

Also,

$$\frac{2\nu^T}{|\nu|^2}\frac{d\nu}{d\theta} = \frac{2}{|f|^2} f^T J^T \frac{d}{d\theta} Jf = \frac{2}{|f|^2} f^T \frac{d}{d\theta} f = \frac{1}{|f|^2}\frac{d}{d\theta}|f|^2 = \frac{d}{d\theta}\ln|f(\phi(\theta))|^2.$$

Therefore,

$$a(\theta) = \operatorname{div} f(\phi(\theta)) - \frac{d}{d\theta}\ln|f(\phi(\theta))|^2. \tag{4.18}$$

Equation (4.18) implies (4.8), since the integral over $[0, \mathcal{T}]$ of the last term on the right hand side of (4.18) is zero. □

4.2 The Poincare map for the fast subsystem

In the present subsection, we analyze the trajectories of the randomly perturbed system (4.2) lying close to the limit cycle $L(y_0)$, $y_0 < y_{bp}$. To this end, we consider an IVP for (4.6) and (4.7) subject to the initial condition:

$$\theta_0 = 0 \quad \text{and} \quad |\xi_0| < \delta. \tag{4.19}$$

Throughout this section, we assume (even when it is not stated explicitly) that $\delta > 0$ is sufficiently small. It will be convenient to view the range of θ_t as $\mathbb{R}^1$ rather than a circle. Equation (4.4) provides the transformation of (θ_t, ξ_t) to the Cartesian coordinates even when θ_t exceeds $\mathcal{T}$.

We now turn to the construction of the Poincare map. Condition $\theta = 0$ defines a transverse crossection of $L(y_0)$, Σ. The trajectory of the deterministic system (4.6) and (4.7) with $\sigma = 0$ returns to Σ in time $\mathcal{T} + O(\xi_0)$. To define the Poincare map for the randomly perturbed system, we also use another transverse crossection $\tilde{\Sigma}$, which is located at an $O(1)$ distance away from Σ. Let (θ_t, ξ_t) be the solution of the IVP (4.6), (4.7), and (4.19) and

$$\tilde{T} = \inf\{t > 0 : (\theta_t, \xi_t) \in \tilde{\Sigma}\}.$$

Definition 4.2. *By the time of the first return of the trajectory (4.6), (4.7), and (4.19) to Σ, we call stopping time T such that*

$$T = \inf\{t > \tilde{T} : \theta_t = \mathcal{T}\}. \tag{4.20}$$

The first return map for (4.6), (4.7), and (4.19) is defined as

$$\bar{\xi} = P(\xi_0), \quad \text{where} \quad \bar{\xi} = \xi_T.$$

In the remainder of this subsection, we compute the linear part of the Poincare map. In the asymptotic expansions below, we omit to indicate the dependence of the remainder terms on $\epsilon > 0$. The latter is assumed to be sufficiently small so that it has no effect on the leading order approximation of the Poincare map.

The following notation is reserved for four functions, which will appear frequently in the asymptotic expansions below:

$$A(t,s) = \exp\{\textstyle\int_s^t a(u)du\}, \quad A(t) = A(t,0),$$
$$B(t,s) = \textstyle\int_s^t A(u,s)b_1(u)du, \quad B(t) = B(t,0).$$

Lemma 4.3. *On a finite time interval $t \in [0, \bar{t}], 0 < \bar{t} < \infty$, the solution of the IVP (4.6), (4.7) and (4.19) admits the following asymptotic expansion*

$$\dot{\theta}_t = \theta_t^{(0)} + \sigma \theta_t^{(0)} + O(\sigma^2, \xi_0^2), \tag{4.21}$$

$$\dot{\xi}_t = \xi_t^{(0)} + \sigma \xi_t^{(1)} + O(\sigma^2, \xi_0^2). \tag{4.22}$$

The leading order coefficients are given by

$$\theta_t^{(0)} = t + \xi_0 B(t) + O(\xi_0^2), \tag{4.23}$$

$$\xi_t^{(0)} = \xi_0 A(t) + O(\xi_0^2). \tag{4.24}$$

26

The first order terms are given by Gaussian diffusion process $z_t = \left(\theta_t^{(1)}, \xi_t^{(1)} \right)^T$:

$$z_t = \int_0^t U(t,s)h(s)dw_s + O(\xi_0), \tag{4.25}$$

where

$$U(t,s) = \begin{pmatrix} 1 & B(t,s) \\ 0 & A(t,s) \end{pmatrix}, \quad h(t) := h(t,0) = (h_1(t,0), h_2(t,0))^T. \tag{4.26}$$

Proof: The procedure for constructing asymptotic expansions of solutions for a class of IVP, which includes (4.6), (4.7) and (4.19) can be found in [2, 19]. These sources also contain the estimates controlling the remainder terms. The coefficients $\theta_t^{(0,1)}$ and $\xi_t^{(0,1)}$ are determined as follows. By plugging in (4.21) and (4.22) into (4.6) and (4.7) and extracting the coefficients multiplying different powers of σ, one obtains IVPs for the functions on the right hand sides of (4.21) and (4.22). Specifically, for the leading order terms we have the following IVP:

$$\dot{\theta}_t^{(0)} = 1 + b_1 \left(\theta_t^{(0)} \right) \xi_t^{(0)}, \tag{4.27}$$

$$\dot{\xi}_t^{(0)} = a \left(\theta_t^{(0)} \right) \xi_t^{(0)}, \tag{4.28}$$

$$\xi_0^{(0)} = \xi_0, \; \theta_t^{(0)} = 0. \tag{4.29}$$

To the next order,

$$\dot{z}_t = \Lambda(t, \xi_0)z_t + h\left(\theta_t^{(0)}, \xi_t^{(0)} \right) dw_s, \tag{4.30}$$

$$z_0 = 0, \tag{4.31}$$

where $z_t = \left(\theta_t^{(0)}, \xi_t^{(1)} \right)^T$, $h = (h_1, h_2)^T$, and

$$\Lambda(t, \xi_0) = \begin{pmatrix} b_1' \left(\theta_t^{(0)}(\xi_0) \right) \xi_t^{(0)}(\xi_0) & b_1 \left(\theta_t^{(0)}(\xi_0) \right) \\ b_1 \left(\theta_t^{(0)}(\xi_0) \right) \xi_t^{(0)}(\xi_0) & a \left(\theta_t^{(0)}(\xi_0) \right) \end{pmatrix}. \tag{4.32}$$

Here, we explicitly indicated the dependence of the leading order coefficients on ξ_0 and used prime to denote the differentiation with respect to θ. Formulae (4.23)-(4.26) in the statement of the lemma follow from (4.27)-(4.32). The details can be found in the appendix to this paper.
□

Next, we calculate the time of the first return.

Lemma 4.4. *The time of the first return is given by*

$$T = T^{(0)} + \sigma T^{(1)} + o(\sigma) + O(\xi_0^2), \tag{4.33}$$

where

$$T^{(0)} = \mathcal{T} - \xi_0 B(\mathcal{T}) + O(\xi_0^2), \tag{4.34}$$

$$T^{(1)} = -\sigma \theta_{\mathcal{T}}^{(1)} = -\sigma \int_0^{\mathcal{T}} [h_1(u) + B(\mathcal{T}, u)h_2(u)] \, dw_u. \tag{4.35}$$

27

Proof : From the definition of the first return time, (4.21), and (4.23), we have

$$T + \xi_0 B(T) + \sigma \theta_T^{(1)} + O(\sigma^2, \xi_0^2) = \mathcal{T} \text{ a.s..} \tag{4.36}$$

Thus,

$$\lim_{\sigma \to 0} T = T^{(0)}(\xi_0) \text{ a.s.,} \tag{4.37}$$

where $T^{(0)}(\xi_0)$ is found from the following equation

$$T^{(0)}(\xi_0) + \xi_0 B\left(T^{(0)}(\xi_0)\right) + O(\xi_0^2) = \mathcal{T}. \tag{4.38}$$

Equation (4.38) implies (4.34). Furthermore, the combination of (4.34), (4.36), and (4.37) yields (4.35).
□

Lemma 4.5. *The first return map is given by the*

$$\bar{\xi} = \mu \xi \left(1 + \sigma r_1\right) + \sigma r_2 + o(\sigma) + O(\xi_0^2), \tag{4.39}$$

where Gaussian RVs $r_{1,2}$ are given by

$$r_1 = -a(0) \int_0^{\mathcal{T}} \left[h_1(u) + B(\mathcal{T}, u)h_2(u)\right] dw_u, \quad r_2 = \int_0^{\mathcal{T}} A(\mathcal{T}, u)h_2(u)dw_u. \tag{4.40}$$

Proof : From (4.22), (4.24)-(4.26), and (4.33), we have

$$\begin{aligned}
\bar{\xi} &= \xi_T = \xi_0 A(T) + \sigma \int_0^T A(T, s)h_2(s)dw_s + O(\sigma^2, \xi_0^2) \\
&= \xi_0 A(T) + \sigma r_2 + O(\sigma^2, \xi_0^2),
\end{aligned} \tag{4.41}$$

where r_2 is defined in (4.40). The first term on the right hand side of (4.41) can be rewritten as follows

$$\begin{aligned}
A(T) &= A(\mathcal{T})A(\mathcal{T} + \sigma T^{(1)}, \mathcal{T}) + o(\sigma) + O(\xi_0) = \mu \exp\left(\sigma a(0)T^{(1)}\right) + o(\sigma) \\
&= \mu \left(1 - \sigma a(0)\theta_{\mathcal{T}}^{(1)}\right) + o(\sigma) + O(\xi_0).
\end{aligned} \tag{4.42}$$

Finally, we extract the expression for $\theta_{\mathcal{T}}^{(1)}$ from (4.25) and (4.26):

$$\theta_{\mathcal{T}}^{(1)} = \int_0^{\mathcal{T}} \left[h_1(u) + B(\mathcal{T}, u)h_2(u)\right] dw_u. \tag{4.43}$$

Equations (4.41)-(4.43) yield (4.39) and (4.40). □

Remark 4.6. We close this section by observing that as follows from (4.40) RV r_1 and r_2 are stochastic integrals of different deterministic functions, say $f(t)$ and $g(t)$ with respect to the same Brownian motion

28

over the interval $[0, \mathcal{T}]$. Consequently, their joint distribution is bivariate normal with 0 mean vector and a covariance matrix that whose diagonal entries are

$$\int_0^{\mathcal{T}} f^2(t)dt \quad \text{and} \quad \int_0^{\mathcal{T}} g^2(t)dt,$$

and the off diagonal entry is

$$\int_0^{\mathcal{T}} f(t)g(t)dt.$$

This is perhaps easiest to see by using Riemann representation of a stochastic integral (see e.g. [42, Proposition 7.6]), basic properties of Brownian motion, and a fact that a random vector is multivariate normal if and only if any linear combination of its components is a normal RV.

4.3   The first return map for the slow variable

Our next goal is to estimate the change of the slow variable, y_t, after one cycle of oscillations of the fast subsystem for the following initial conditions:

$$0 < y_{bp} - y_0 = O(1), \ x_0 = \phi(0) + \xi_0 \nu(0) \in \Sigma, \ \text{and} \ |\xi_0| < \delta. \tag{4.44}$$

We denote the first return map for y by

$$\bar{y} = P(y, \xi_0), \quad \text{where} \quad P(y_0, \xi_0) = y_T,$$

and T is the first return time of the fast subsystem (see Definition 4.2).

Lemma 4.7. *The first return map for y has the following form:*

$$P(y, \xi) = y + \epsilon G(y) + \epsilon \sigma r_3 + \epsilon a \xi + o(\epsilon \sigma), \tag{4.45}$$

where

$$G(y) = \int_0^{\mathcal{T}} g\left(\phi(s), y\right) ds \tag{4.46}$$

and $r_3 = N\left(0, O(1)\right)$ and a is a constant independent of σ and ϵ.

Remark 4.8. Recall that $\mathcal{T}$ and $\phi(\cdot)$ are functions of slow variable y (see (2.2)). To avoid using cumbersome notation we continue to suppress the dependence on y.

Proof : By (2.10),

$$y_T = y_0 + \epsilon \int_0^T g(x_s, y_0)ds + O(\epsilon^2), \tag{4.47}$$

where x_s satisfies IVP (4.6), (4.7), and (4.19). Let $x = \phi(\theta) + \xi \nu(\theta)$ and denote

$$\tilde{g}(\theta, \xi, y) := g(x, y), \ g_0(s) = \tilde{g}(s, 0), \ g_1(s) = \frac{\partial \tilde{g}}{\partial \theta}(s, 0), \ \text{and} \ g_2(s) = \frac{\partial \tilde{g}}{\partial \xi}(s, 0). \tag{4.48}$$

29

Using (4.48), we rewrite (4.47) as

$$y_T = y_0 + \epsilon \int_0^T \tilde{g}(\theta_s^{(0)} + \sigma\theta_s^{(1)}, \xi_s^{(0)} + \sigma\xi^{(1)}) + O(\epsilon\sigma^2). \tag{4.49}$$

Using the Taylor expansion for $\tilde{g}$ in (4.49) and (4.21), (4.22) and (4.33), from (4.49) we derive

$$
\begin{aligned}
y_T &= y_0 + \epsilon \int_0^{\mathcal{T}} \left\{ g_0(s) + g_1(s)\left[\xi_0 B(s) + \sigma\theta_s^{(1)}\right] + g_2(s)\left[\xi_0 A(s) + \sigma\xi_s^{(1)}\right] \right\} ds \\
&\quad + \int_{\mathcal{T}}^{\mathcal{T} - \xi_0 B(\mathcal{T}) - \sigma\theta_{\mathcal{T}}^{(1)}} g_0(s)ds + o(\epsilon\sigma) + O(\epsilon\xi_0^2).
\end{aligned} \tag{4.50}
$$

We approximate the last integral on the right hand side of (4.50) by

$$\int_{\mathcal{T}}^{\mathcal{T} - \xi_0 B(\mathcal{T}) - \sigma\theta_{\mathcal{T}}^{(1)}} g_0(s)ds = -g_0(0)\left[\xi_0 B(\mathcal{T}) + \sigma\theta^{(1)}\right] + o(\sigma, \xi_0). \tag{4.51}$$

The combination of (4.50) and (4.51) implies (4.45) with

$$
\begin{aligned}
a &= \int_0^{\mathcal{T}} \left[g_1(s)B(s) + g_2(s)A(s)\right] ds - g_0(0)B(\mathcal{T}), \tag{4.52} \\
r_3 &= \int_0^{\mathcal{T}} \left[g_1(s)\theta_s^{(1)} + g_2(s)\xi_s^{(1)}\right] ds. \tag{4.53}
\end{aligned}
$$

$\square$

4.4 The exit problem

In the present subsection, we first combine the return maps derived for the slow and fast subsystems to obtain the Poincare map for the full three-dimensional system. Next, we approximate the Poincare map and the BA of the limit cycle $L(y_c)$ and characterize the distribution of the exit times for the approximate problem. This distribution is then related to the distribution of the number of spikes within bursting episodes. To approximate the Poincare map we linearize it around the stable fixed point of the deterministic map corresponding to the limit cycle $L(y_c)$. Aside from the systematic derivation of the Poincare map in the previous subsections, we offer no rigorous justification for substituting the nonlinear Poincare map with its linear part in the analysis of the exit problem. While in general, such approximation may not be accurate, we believe that for the present problem, the analysis of the linearized system captures the statistics of the first exit times well for the following reason. In models of square wave bursting the limit cycle generating spiking is often located close to the boundary of its BA (see Fig. 6b for a representative example). Therefore, before the trajectories leave the BA, they remain in a small neighborhood of the limit cycle, where the linear part of the vector field governs the dynamics. After these preliminary remarks, we turn to the derivation of the approximate problem and its analysis.

Lemmas 4.5 and 4.7 yield the asymptotic formulae for the first return map of the randomly perturbed system (2.9) and (2.10) in the normal coordinates (4.4):

$$\xi_{n+1} = \mu\xi_n\left(1 + \sigma r_{1,n}\right) + \sigma r_{2,n} + o(\sigma), \tag{4.54}$$

$$y_{n+1} = y_n + \epsilon G(y_n) + \epsilon\sigma r_{3,n} + \epsilon a\xi_n + o(\epsilon\sigma), \; n = 0, 1, 2, \ldots, \tag{4.55}$$

where (ξ_0, y_0) are given in (4.44) and the expressions for a and $r_{i,n}$, $i = 1, 2, 3$ are are given in (4.40),(4.52), and (4.53). Recall that by (SS) (see Section 2), $G(y)$ has a simple zero at $y = y_c$ and $\lambda := -G'(y_c) > 0$. Thus, $(0, y_c)$ is an attracting fixed point of the unperturbed map (4.54) and (4.55) with $\sigma = 0$. The linearization of (4.54) and (4.55) about $(0, y_c)$ yields

$$\xi_{n+1} = \mu\xi_n\left(1 + \sigma\tilde{r}_{1,n}\right) + \sigma\tilde{r}_{2,n}, \tag{4.56}$$

$$\eta_{n+1} = \lambda\eta_n + \epsilon\sigma\tilde{r}_{3,n} + \epsilon a_2\xi_n, \quad n = 0, 1, 2, \ldots, \tag{4.57}$$

where $\eta = y - y_c$, $0 < \lambda = 1 - \epsilon a_1$, and $0 < \mu < 1$. The distributions of the RVs $r_{i,n}$, $i = 1, 2, 3$ depend on y_n, as both the upper bound of integration $\mathcal{T}$ and the integrands in (4.40) and (4.53) are smooth functions of y. The stochastic terms $\tilde{r}_{i,n}$, $i = 1, 2, 3$ in the linearized system are obtained by evaluating the expressions for $\tilde{r}_{i,n}$, $i = 1, 2, 3$ in (4.40) and (4.53) at $y = y_c$. Thus, $(\tilde{r}_{1,n}, \tilde{r}_{2,n}, \tilde{r}_{3,n})$ are IID copies of a $N(0, \Sigma_3)$, where the entries of Σ_3 are $O(1)$ in a sense that they do not depend on any other parameters. Further, we approximate the BA of $L(y_c)$ by a cylindrical shell, so that in (ξ, η) coordinate plane, it projects to $\Pi := \left[-\tilde{h}_\xi, h_\xi\right] \times \left[-\tilde{h}_\eta, h_\eta\right]$ for some $\tilde{h}_{\xi,\eta} > h_{\xi,\eta} > 0$ independent of $\sigma > 0$. Each iteration of the Poincare map corresponds to a spike within a burst. The burst terminates when the trajectory leaves the BA of $L(y_c)$. Assuming that the linearization (4.56) and (4.57) and Π provide suitable approximations for the Poincare map and the BA of $L(y_c)$ respectively, the distribution of the number of spikes in one burst can be approximated by the distribution of the first exit times for the trajectories of (4.56) and (4.57) from Π:

$$\tau = \min\{\tau_\xi, \tau_\eta\}, \tag{4.58}$$

where

$$\tau_\xi = \inf_{n>0}\{\xi_n > h_\xi\} \quad \text{and} \quad \tau_\eta = \inf_{n>0}\{\eta_n > h_\eta\}.$$

We are now in a position to apply the the results of Section 3 to describe the distribution of (4.58). By Theorem 3.7, the distribution of τ is asymptotically geometric with parameter

$$p \approx \frac{\sigma}{C\sqrt{2\pi}}e^{-\frac{C}{\sigma^2}} \tag{4.59}$$

for some $C > 0$ independent of ϵ and σ. In the proof of Theorem 3.7, we studied a class of $2D$ randomly perturbed maps that includes (4.56) and (4.57). However, the distribution of τ is effectively determined by the first equation (4.56), i.e. by the $1D$ first return map of the fast subsystem. This can be seen by observing that according to the approximations given at the end of proof of Theorem 3.7 (see the arguments following (3.30)) if $\epsilon > 0$ is sufficiently small then $\tau_\xi \ll \tau_\eta$ and $\tau \sim \tau_\xi$. Thus, in type I models the distribution of spikes in one burst is effectively determined by the $1D$ first return map for the fast subsystem (4.56). In particular, the statistics of the number of spikes in one burst does not depend on the relaxation parameter $\epsilon > 0$, provided the latter is sufficiently small.

4.5 Type II model

The derivation of the Poincare map for the type II models differs from the analysis in Sections 4.1-4.4 for type I models only in some minor details. In this subsection, we comment on the necessary modifications and state the final result. Recall that in contrast to type I models, in (2.11) and (2.12), stochastic forcing enters the slow equation. As before, the initial condition is given by (4.44). On finite time intervals, solutions of the IVP for (2.11) and (2.12) admit the following asymptotic expansions

$$x_t = x_t^{(0)} + \epsilon\sigma x_t^{(1)} + O\left((\epsilon\sigma)^2\right), \tag{4.60}$$

$$y_t = y_t^{(0)} + \epsilon\sigma y_t^{(1)} + O\left((\epsilon\sigma)^2\right). \tag{4.61}$$

where the first order corrections $x_t^{(1)}$ and $y_t^{(1)}$ are Gaussian processes (cf. Theorem 2.2 [19]). Using (4.60) and (4.61), we obtain the leading order approximation of the fast subsystem:

$$\dot{x}_t = f(x_t, y_0) + \epsilon\sigma\frac{\partial f(x_t^{(0)}, y_0)}{\partial y}y_t^{(1)} + o(\epsilon\sigma). \tag{4.62}$$

From this point, the derivation of the Poincare map follows the same lines as we described in detail for type I models in Sections 4.1-4.4. We omit any further details and state the final result, the linear approximation of the Poincare map for the present case:

$$\xi_{n+1} = \mu\xi_n\left(1 + \epsilon\sigma\tilde{r}_{1,n}\right) + \epsilon\sigma\tilde{r}_{2,n}, \tag{4.63}$$

$$\eta_{n+1} = \lambda\eta_n + \epsilon\sigma\tilde{r}_{3,n} + \epsilon a_2\xi_n, \quad n = 0, 1, 2, \ldots, \tag{4.64}$$

As in the previous case, we are interested in the distribution of the first exit time τ (see (4.58)). To estimate the latter, we use the same argument as in the previous subsection. This time the system is described by

$$\Theta_{n+1} = A_{n+1}\Theta_n + \sigma\epsilon G_{n+1}, \quad n \geq 1, \tag{4.65}$$

where A_n is as before and $G_n = \begin{bmatrix} r_{2,n} \\ r_{3,n} \end{bmatrix}$. The presence of the factor ϵ in both components of G_n leads to the following expression for the numerator of p (see (3.27)):

$$\mathbb{P}\left(\frac{\mu X_1 r_1 + r_2}{\sigma_{X_1}} > \frac{h_1 - \mu X_1}{\epsilon\sigma\sigma_{X_1}}, r_3 > \frac{h_2 - a_2 X_1}{\sigma} + \frac{\lambda(h_2 - X_2)}{\epsilon\sigma}, (X_1, X_2) \in B_h\right).$$

This expression decays very fast as a function of $h_2 - X_2$ and since X_2 has heavy tails it is approximated (up to inessential polynomial factors) by

$$\mathbb{P}\left(\frac{\mu X_1 r_1 + r_2}{\sigma_{X_1}} > \frac{h_1 - \mu X_1}{\epsilon\sigma\sigma_{X_1}}, r_3 > \frac{h_2 - a_2 X_1}{\sigma}, (X_1, X_2) \in B_h\right).$$

We are now in the analogous situation to that encountered in (3.28), except that the small parameter $\epsilon > 0$ appears in the denominator of the other variable. As a consequence, this time we obtain that $\tau_\xi \ll \tau_\eta$ for small $\epsilon > 0$. Therefore, in contrast to type I models, the escape of a trajectory of (2.11) and (2.12) from $\mathcal{A}$ is dominated by the slow subsystem, i.e., $\tau = \tau_\eta$.

5 Numerical example

In the present section, we illustrate the statistical regimes identified in this study with numerical simulations of a conductance based model of a neuron in the presence of noise. To this end, we use a three variable model of a bursting neuron introduced by Izhikevich [26]. The model dynamics is driven by the interplay of the three ionic currents: persistent sodium, I_{NaP}, the delayed rectifier, I_K, a slow potassium M-current, I_{KM}, and a passive leak current I_L. The following system of three differential equations describes the dynamics of the membrane potential, v, and two gating variables n and y:

$$C\dot{v} = F(v, n, y), \tag{5.1}$$

$$\tau_n \dot{n} = n_\infty(v) - n, \tag{5.2}$$

$$\tau_y \dot{y} = y_\infty(v) - y, \tag{5.3}$$

where $F(v, n, y) = -g_{NaP}m_\infty(v)(v - E_{NaP}) - g_K n(v - E_K) - g_{KM}y(v - E_K) - g_L(v - E_L) + I$; g_s and E_s, are the maximal conductance and the reversal potential of I_s, $s \in \{NaP, K, KM, L\}$, respectively; and I is the applied current. The time constants τ_n and τ_y determine the rates of activation in the populations of K and KM channels. The steady-state functions are defined by $s_\infty(v) = \left(1 + \exp\left(\frac{a_s - v}{b_s}\right)\right)^{-1}$, $s \in \{m, n, y\}$. The parameter values are given in the caption to Fig. 7. This completes the description of the deterministic model. The random perturbation is used in the form of white noise, $\sigma\dot{w}_t$ and is added to the first equation (5.1) for type I model or to the third one (5.3) for type II model. After suitable rescaling, these models can be put in the nondimensional form (2.9), (2.10) or (2.11), (2.12). The separation of the timescales in the nondimesional models (i.e. small $\epsilon >$)) is the result of the presence of the disparate time constants $\tau_h \gg \tau_n$ in the original model (see caption to Fig. 7).

The parameters of the deterministic system are chosen so that it has a limit cycle located as shown in Fig. 3c. In the presence of small noise the system generates bursting. In each numerical experiment, we integrated the randomly perturbed system using the Euler-Maruyama method [24] until it generated $5,000$ bursts. We used these data to estimate the probability density for the number of spikes within one burst. In Fig. 7, we plot the histograms for the number of spikes in one burst for type I and type II models. The histograms in Fig. 7 are scaled to approximate the probability density function (PDF) for the number of spikes in one burst. Both PDFs shown Fig. 7a,b have distinct exponential tails as expected for the asymptotically geometric RVs. Note that the distribution in Fig. 7a fits well with the geometric distribution for $N > 100$, while in Fig. 7b the geometric distribution fits the data almost on the entire domain $N > 10$. In addition, the peak in the histogram in Fig. 7a is reminiscent of the PDF characteristic for the diffusive escape (see Fig. 5). For comparison, we plotted a slightly shifted diffusive PDF, $\Psi_a(x)$, $a = 10.8$ in Fig. 7a. Matching the data and Ψ_a is a delicate matter, because it is not clear how wide is the range of n, to which the estimates of Theorem 3.9 apply. Nonetheless, the qualitative similarity of the peak in the histogram in the range $n \sim 50 - 100$ and the diffusive PDF is apparent. We repeated these numerical experiments for a few other sets of parameters and found qualitatively similar results.

Collecting the statistical data shown in Fig. 7 requires integrating the system over very long intervals of time, for which it would be hard to justify the accuracy of the Euler-Maruyama method. However, capturing the statistical features of the dynamical patterns does not require having an accurate solution on the entire interval of time, because they are determined by the discrete dynamics of the first return map. The
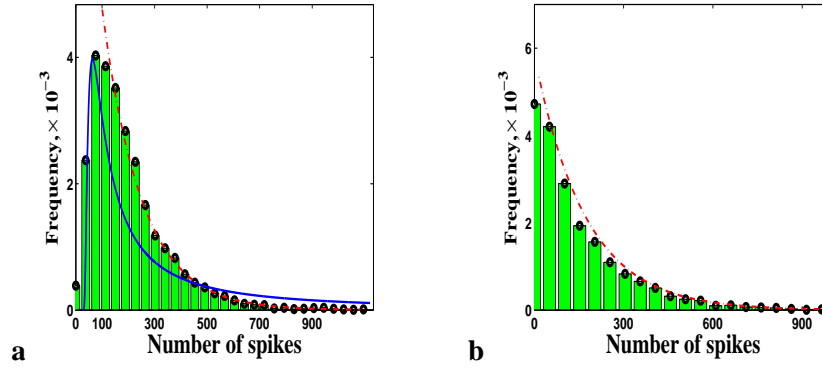
Figure 7: The histograms for the number of spikes in one burst. The histograms computed for the type I model in (a) and type II in (b) are normalized to approximate the corresponding PDFs. The tails of both functions are well approximated by the exponential densities with parameters 0.0067 and 0.0125 respectively. In (b) the exponential distribution already gives a very good approximation for the number of spikes exceeding 10. The region of exponential behavior in (a) starts around $n \sim 100$. In (a), we also plotted in solid blue line the shifted diffusive density $\Psi_a(x - 25), a \approx 10.8$. Although it is hard to claim a quantitative fit of the diffusive density and the data, the qualitative similarity between the diffusive pdf $\Psi_a(x)$ and the peak in the data in the range $n \sim 50 - 100$ is apparent. The values of parameters are $C = 1 \left(\mu F cm^{-2}\right)$; $g_{NA} = 20$, $g_K = 10$, $g_{KM} = 5$, $g_L = 8 \left(mScm^{-2}\right)$; $E_{Na} = 60$, $E_K = -90$, $E_L = -80$ (mV); $a_m = -20$, $a_n = -25$, $a_y = -10$ (mV); $b_m = 15$, $b_n = 5$, $b_y = 5$; $\tau_n = 0.152$, $\tau_y = 20 \left(ms^{-1}\right)$, $I = 5pA$, and $\sigma = 1$.

iterations of the latter are expected to be insensitive to the numerical noise as suggested by the analysis of the randomly perturbed maps in Section 3. Therefore, we only need to have accurate numerical solutions on the time intervals comparable with the typical periods of the fast oscillations. This is easy to achieve with the Euler-Maruyama method. We repeated these numerical experiments using the second order Runge-Kutta method and obtained very similar results. These informal arguments form the rationale for using the above numerical scheme. The rigorous justification of the numerics is beyond the scope of this paper.

Apendix

In this appendix, we provide the details of the derivation of (4.23)-(4.26), which were omitted in the main part of the paper.

To derive (4.23) and (4.24), we first note that $\theta_t^{(0)}$ is a monotonic function on $[0, \bar{t}]$, provided $\delta > 0$ is sufficiently small. Thus,

$$\frac{d\xi^{(0)}}{d\theta^{(0)}} = a(\theta^{(0)})\xi^{(0)} + O(\xi_0^2),$$

and

$$\xi^{(0)}(\theta^{(0)}) = \xi_0 A(\theta^{(0)}) + O(\xi_0^2). \tag{A.1}$$

By plugging in (A.1) into (4.27), we have

$$\dot{\theta}_t^{(0)} = 1 + b_1(\theta_t^{(0)})\xi_0 A(\theta^{(0)}). \tag{A.2}$$

By Gronwall's inequality,

$$\theta_t^{(0)} = \psi_t + O(\xi_0^2), \ t \in [0, \bar{t}], \tag{A.3}$$

where ψ_t solves

$$\dot{\psi}_t^{(0)} = 1 + \xi_0 b_1(t)A(t), \ \psi_0 = 0. \tag{A.4}$$

The combination of (A.1), (A.3), and (A.4) implies (4.24).

We next turn to IVP (4.30), (4.31) and (4.24). Let $U(t, \xi_0)$ denote the principal matrix solution of the homogeneous system

$$\dot{z}_t = \Lambda(t, \xi_0)z_t. \tag{A.5}$$

Then the solution of (4.30) and (4.31) is given by

$$z_t = \int_0^t U(t, s, \xi_0)h\left(\theta_s^{(0)}, \xi_s^{(0)}\right) dw_s = \int_0^t U(t, s)h(s, 0) dw_s + O(\xi_0), \ t \in [0, \bar{t}], \tag{A.6}$$

where

$$U(t, s, \xi_0) = U(t, \xi_0)U^{-1}(s, \xi_0) \quad \text{and} \quad U(t, s) = U(t, s, 0). \tag{A.7}$$

Finally, by integrating (A.5) with $\xi_0 = 0$ and appropriate initial conditions, one computes

$$U(t,0) = \begin{pmatrix} 1 & B(t) \\ 0 & A(t) \end{pmatrix}. \tag{A.8}$$

The expression for $U(t,s)$ in (4.26) follows from (A.7) and (A.8).

References

[1] J.P. Baltanas and J.M. Casado, Bursting behavior, of the FitzHugh-Nagumo neuron model subject to monochromatic noise, *Physica D*, **122**, 231–240, 1998.

[2] Yu.N. Blagoveshchenskii, Diffusion processes depending on small parameter, *Theory of Probability and Its Applications*, **VII**(2), 130–146, 1962.

[3] N. Berglund and B. Gentz, *Noise-Induced Phenomena in Slow-Fast Dynamical Systems: A Sample-Paths Approach*, Springer, 2006.

[4] J. Best, A. Borisyuk, J. Rubin, D. Terman and M. Wechselberger, The dynamic range of bursting in a model respiratory pacemaker network, *SIAM J. Appl. Dyn. Syst.*, **4**, 1107-1139, 2005.

[5] R. J. Butera, J. Rinzel, and J. C. Smith, Models of respiratory rhythm generation in the pre-Botzinger complex: I. Bursting pacemaker neurons, *Journal of Neurophysiology*, **82**, 382-397, 1999.

[6] T.R. Chay, Chaos in a three-variable model of an excitable cell, *Physica D*, **16**, 233-242, 1985.

[7] T.R. Chay and J. Rinzel, Bursting, beating, and chaos in an excitable membrane model, *Biophys. J.*, **47**, 357–366, 1985.

[8] C. Chow and J. White, Sponteneous action potentials due to channel fluctuations, *Biophys. J.*, **71**, 3013-3021, 1996.

[9] J.J. Collins, C.C. Chow, and T.T. Imhoff, Aperiodic stochastic resonance in excitable systems, *Phys. Rev. E*, **52**(4), R3321–R3324, 1995.

[10] R.E.L. DeVille, C. Muratov, and E. Vanden-Eijnden, Two distinct mechanisms of coherence in randomly perturbed dynamical systems, *Physical Review E*, **72**, 031105, 2005.

[11] J. L. Doob. *Stochastic Processes*, Reprint of the 1953 original, Wiley, 1990.

[12] P. Embrechts and C.M. Goldie, Perpetuities and random equations, in *Asymptotic statistics*, 75–86, Physica, Heidelberg, 1994.

[13] W. Feller, *An Introduction to Probability Theory and Its Applications*, vol. I. Wiley, 3rd edition, 1968.

[14] N. Fenichel, Persistence and smoothness of invariant manifolds for flows, *Indiana Univ. Math. J.*, **21**, 193-226, 1971/1972.

[15] R.F. Fox, Stochastic versions of the Hodgkin-Huxley equations, *Biophys. J.*, **72**(5), pp. 2068–2074.

[16] R.F. Fox and Y. Lu, Emergent collective behavior in large numbers of globally coupled independently stochastic ion channels, *Phys. Rev. E*, **49**(5), pp. 3421–3431.

[17] M.I. Freidlin, On stable oscillations and equilibriums induced by small noise, *J. of Stat. Phys.*, **103**(1-2), 283–300, 2001.

[18] M.I. Freidlin, On stochastic perturbations of dynamical systems with fast and slow components, *Stochastics and Dynamics*, **1**(2), 261–281, 2001.

[19] M.I. Freidlin and A.D. Wentzell, *Random perturbations of dynamical systems*, 2nd ed., Springer, New York, 1998.

[20] R. Ghigliazza and P. Holmes, Minimal models of bursting neurons: The effects of multiple currents, conductances and timescales, *SIAM J. on Appl. Dyn. Syst.*, 3 (4), 636-670, 2004.

[21] C.M. Goldie, Implicit renewal theory and tails of solutions of random equations, *The Annals of Applied Probability*, $\mathbf{1}$(1), 126–166, 1991.

[22] J. Guckenheimer and P. Holmes, *Nonlinear Oscillations, Dynamical Systems, and Bifurcations of Vector Fields*, Springer, 1983.

[23] J. Hale, *Ordinary Differential Equations*, second edition, R.E. Krieger Publishing Company, 1980.

[24] D.J. Higham, An algorithmic introduction to numerical simulation of stochastic differential equations, *SIAM Rev.*, $\mathbf{43}$(3), pp. 525–546, 2001.

[25] A.A. Hill, J. Lu, M.A. Massino, O.H. Olsen, and R.L. Calabrese, A model of a segmental oscillator in the leech heartbeat neuronal network, *J. Comp. Neurosci.*, $\mathbf{10}$, 281–302, 2001.

[26] E.M.Izhikevich, *Dynamical Systems in Neuroscience: The Geometry of Excitability and Bursting*, The MIT Press, Boston, MA, 2007.

[27] C.K.R.T. Jones, Geometric singular perturbation theory, Lecture Notes in Mathematics, Vol. 1609, Springer, Berlin, pp. 44-118, 1995.

[28] N. L. Johnson and S. Kotz. *Discrete Distributions*. Wiley, 1969.

[29] H. Kesten, Random difference equations and renewal theory for products of random matrices, *Acta Math.*, $\mathbf{131}$, 207–248, 1973.

[30] S. Kwapień and W. A. Woyczyński. *Random Series and Stochastic Integrals: Single and Multiple* Birkhäuser, 1992.

[31] E. Lee and D. Terman, Uniqueness and stability of periodic bursting solutions, *JDE*, $\mathbf{158}$, 48–78, 1999.

[32] A. Longtin and K. Hinzer, Encoding with bursting, subthreshold oscillations, and noise in mammalian cold receptors, *Neural Computation*, $\mathbf{8}$(2), 215–255, 1996

[33] G.S. Medvedev, Transition to bursting via deterministic chaos, *Phys. Rev. Lett.*, 97, 048102, 2006.

[34] G.S. Medvedev, Reduction of a model of an excitable cell to a one-dimensional map, *Physica D*, $\mathbf{202}$, 37-59, 2005.

[35] G.S. Medvedev and J.E. Cisternas, Multimodal regimes in a compartmental model of the dopamine neuron, *Physica D*, $\mathbf{194}$, 333-356 , 2004.

[36] L. S. Pontryagin and L. V. Rodygin, Approximate solution of a system of ordinary differential equations involving a small parameter in the derivatives, *Soviet. Math. Dokl.*, $\mathbf{1}$, 237–240, 1960.

[37] J. Rinzel, A formal classification of bursting mechanisms in excitable systems, in A.M. Gleason, ed., Proc. of the Intern. Congress of Mathematicians, AMS, 135–169, 1987.

[38] J. Rinzel and G.B. Ermentrout, Analysis of neural excitability and oscillations, in C. Koch and I. Segev, eds *Methods in Neuronal Modeling*, MIT Press, Cambridge, MA, 1989.

[39] P.F. Rowat and R.C. Elson, State-dependent effects of Na channel noise on neuronal burst generation, *J. Comp. Neurosci.*, **16**, pp. 87–112, 2004.

[40] J. Rinzel and W.C. Troy, A one-variable map analysis of bursting in the Belousov-Zhabotinskii reaction, in: J.A. Smoller, ed. *Nonlinear Partial Differential Equations*, AMS, Providence, 411–427, 1982

[41] G. Smith, Modeling the stochastic gating of ion channels, in C.P. Fall et al, editors: *Computational Cell Biology*, Interdisciplinary Applied Mathematics, vol. 20, Springer, 2002.

[42] J.M. Steele. *Stochastic Calculus and Financial Applications* Springer-Verlag, 2001.

[43] J. Su, J. Rubin, and D. Terman, Effects of noise on elliptic bursters, *Nonlinearity*, **17**, 133-157, 2004.

[44] D. Terman, The transition from bursting to continuous spiking in excitable membrane models, *J. Nonl. Sci.*, **2**, 135–182, 1992.

[45] W. Vervaat, On a stochastic difference equation and a representation of nonnegative infinitely divisible random variables, *Adv. in Appl. Probab.*, **11**(4) 750–783, 1979.

[46] J. White, J. Rubenstein, and A. Kay, Channel noise in neurons, *Trends in Neurosci.*, **23**(3), 131–137, 2000.

[47] V.A. Zorich, Mathematical Analysis II, Springer, 2004.